INFORMATION TO USERS

This manuscript has been reproduced from the microfilm master. UMI films the text directly from the original or copy submitted. Thus, some thesis and dissertation copies are in typewriter face, while others may be from any type of computer printer.

The quality of this reproduction is dependent upon the quality of the copy submitted. Broken or indistinct print, colored or poor quality illustrations and photographs, print bleedthrough, substandard margins, and improper alignment can adversely affect reproduction.

In the unlikely event that the author did not send UMI a complete manuscript and there are missing pages, these will be noted. Also, if unauthorized copyright material had to be removed, a note will indicate the deletion.

Oversize materials (e.g., maps, drawings, charts) are reproduced by sectioning the original, beginning at the upper left-hand corner and continuing from left to right in equal sections with small overlaps.

Photographs included in the original manuscript have been reproduced xerographically in this copy. Higher quality 6" x 9" black and white photographic prints are available for any photographs or illustrations appearing in this copy for an additional charge. Contact UMI directly to order.

Bell & Howell Information and Learning
300 North Zeeb Road, Ann Arbor, MI 48106-1346 USA
800-521-0600

Université d'Ottawa · University of Ottawa

Transition Metal Guanidinate Complexes of Groups 4 and 5

Thesis submitted to the
School of Graduate Studies and Research
University of Ottawa
In partial fulfillment of the requirements for the
M. Sc. Degree in the
Ottawa-Carleton Chemistry Institute

Supervisor: Professor Darrin S. Richeson

National Library
of Canada

Acquisitions and
Bibliographic Services

395 Wellington Street
Ottawa ON K1A 0N4
Canada

Bibliothèque nationale
du Canada

Acquisitions et
services bibliographiques

395, rue Wellington
Ottawa ON K1A 0N4
Canada

Your file Votre référence

Our file Notre référence

0-612-46620-5

Canada

This thesis is dedicated to the one person who stood by me always.

To my wife, Christine.

Thesis Abstract

Following the introduction/literature review section (chapter 1) the body of this thesis begins. The reaction of $LiN(SiMe_3)_2$ with RNCNR [R = ^{i}Pr, Cy] resulted in formation of the new tetra substituted guanidinate ligands $Li(RN)_2CN(SiMe_3)_2$. Chapter 2 describes the reactions of these ligands with MCl_4 [M = Zr, Hf] to give $Cl_2M[(RN)_2CN(SiMe_3)_2]_2$ or $[Cl_4M(CyN)_2CN(SiMe_3)_2]^-$ depending on the metal ligand ratio employed. Reaction of $[Cl_4Zr(CyN)_2CN(SiMe_3)_2]^-$ with 3 equivalents of BzMgCl gave the first example of an organo-zirconium complex supported by a guanidinate ligand. Single crystal x-ray analysis of these complexes confirmed the bonding features of these ligands.

Chapter 3 reports on the reaction between triisopropyl guanidine $(^iPrN)C(NH^iPr)_2$ and group 5 metal alkyl precursors such as Me_3TaCl_2 and Me_2NbCl_3. These species react by protonation/elimination of metal bonded chloride groups and incorporation of a monoanionic guanidinate ligand. The major isolated products of these are $Me_3TaCl[(^iPrN)_2C(NH^iPr)]$ and $Me_2NbCl_2[(^iPrN)_2C(NH^iPr)]$ and have been attributed to the result of HCl elimination. Single crystal x-ray analysis of these complexes confirmed the bonding features of the triisopropyl guanidinate ligand. $MeNbCl_3[(^iPrN)_2C(NH^iPr)]$ was also isolated in trace amounts and crystallographically characterized. Both Ta and Nb species react with MeLi to yield $Me_4Ta[(^iPrN)_2C(NH^iPr)]$ and $Me_3NbCl[(^iPrN)_2C(NH^iPr)]$.

Reactions of triisopropyl guanidine with $ZrBz_4$ and $ZrCl_4$ are reported in chapter 4. The products isolated from these reactions are $Bz_2Zr[(^iPrN)_2C(NH^iPr)]_2$ or the mixture $Cl_3Zr[(^iPrN)_2C(NH^iPr)]$ + $(^iPrNH)_3CCl$ regardless of the stiochiometry employed. When the mixture containing $Cl_3Zr[(^iPrN)_2C(NH^iPr)]$ and $(^iPrNH)_3CCl$ was reacted with BzMgCl the organic soluble complex $BzClZr[(^iPrN)_2C(NH^iPr)]_2$ was be generated.

Also reported in chapter 4 are the results obtained when the dilithium salt of triisopropyl guanidine was reacted with $ZrCl_4$. Triisopropyl guanidine reacts with 2 equivalents of MeLi to form a reagent that acts as $(^iPrN)_3CLi_2$. The reaction of this species with $ZrCl_4$ yielded a unique dimer $[Cl_2Zr(^iPrN)_3C]_2$ which possessed a bridging dianionic guanidinate ligand. Preliminary reactions of this dimer with ethylene and propylene in the presence of MAO showed encouraging catalytic properties.

Acknowledgements

Many people have helped me during my time as a graduate student. I would first like to thank my wife, Christine. Without her years of support, I would not have been able to obtain this degree. Thanks to my supervisor, Dr. Darrin Richeson, who gave me the opportunity to study here and learn from a great man with seemingly infinite chemistry knowledge. Thanks to Dr. Glenn Yap for all of my crystal structure data, Dr. Glenn Facey for some 500 MHz NMR experiments, Vladimir Kuznetsov for my elemental analysis and finally, to the members of my group who made obtaining this degree fun.

Table of Contents

List of Figures

List of Tables

List of abbreviations

NMR	Nuclear Magnetic Resonance	ppm	Parts per million
THF	Tetrahydofuran	ORTEP	Oak Ridge Thermal Ellipsoid Program
^{i}Pr	Isopropyl	Cy	Cyclohexyl
Ph	Phenyl	Cp	Cyclopentadienyl
Me	Methyl	Py	Pyridine
g	Grams	MHz	Mega Hertz
mmol	Millimole	ml	Milliliter
R	General alkyl	X	General halogen
MAO	Methyl aluminoxane	Bz	Benzyl
M	General metal	TMM	Trimethylene methane
p	para	L_n	General ligand
EA	Elemental analysis	cod	Cyclooctadiene
m	Multiplet	br	broad
t	Triplet	s	singlet
sept	Septet	q	quartet
Å	Angstrom	Et	Ethyl
d	Doublet	M	Molarity
°	Degree	XRD	X-ray diffraction

Chapter 1

Introduction and Literature Review

Introduction

Guanidines [RN=C(NHR)$_2$] bear the same relationship to carbonic acid as amidines do to carboxylic acids (Scheme 1). Amidines and their deprotonated anions are frequently encountered in both bridging and chelating coordination modes and are now firmly established as flexible ligands capable of coordination to a wide variety of metal centers. Guanidines (the amino substituted amidine) may be more promising, potentially being stronger electron donors than amidines and apparently possessing all the coordination possibilities of amidines. The potential for even richer coordination chemistry arises from the presence of the third nitrogen atom. Furthermore there exists the possibility of a second deprotonation to provide a dianionic ligand $[C(NR)_3]^{2-}$ (the nitrogen analogue of carbonate) which is unavailable to the carboxylic acid analogues.

Our initial interest in exploiting the potential of guanidines and their anions as ligands was prompted by the prospect that the dianion might exhibit an η^3 coordination mode in which all three nitrogen donors are bound to a single metal ion. However, our main goal was to extend the limited knowledge of guanidine transition metal chemistry with views to perhaps be able to generalize and predict future chemistry. Many substitution patterns are available for guanidines. For example, by substituting hydrogen in the parent species [$(H_2N)_2CNH$] for an alkyl group, mono, di, tri, tetra and finally penta substituted guanidines results [$(R_2N)_2CNR$] (R = alkyl, H) (Scheme 2). Given this variety guanidines represent an ideal system for exploring the effects of changing the steric bulk and electronic properties of this ligand on the product compounds. Modification of the organic substituents on the nitrogen atoms allow for making rational modifications that can be tuned to stabilize desired

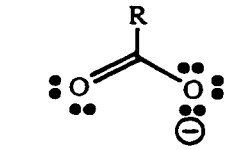

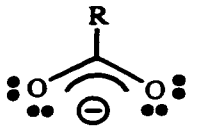

carboxylate

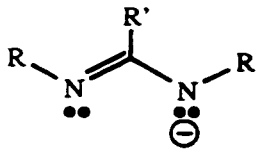

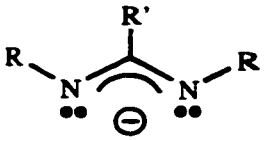

amidinate
R' = H, alkyl, aryl

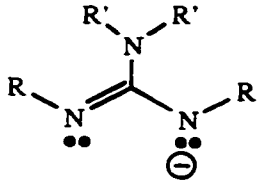

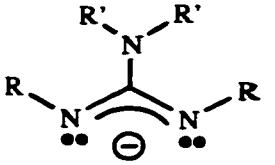

guanidinate
R' = H, alkyl, aryl, or combination

Scheme 1

Trisubstituted

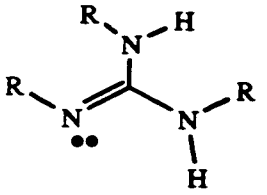

N, N', N"
1, 2, 3

Tetrasubstituted

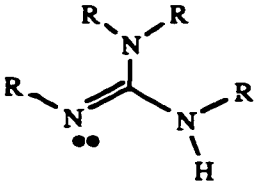

N, N, N', N"
1, 1, 2, 3

Scheme 2

structural and reactivity characteristics. The use of guanidine ligands to accomplish these goals has received limited attention in inorganic coordination and organometallic chemistry.

The most obvious feature that arises from changes to R is the ability to change the size/sterics of substituents on the nitrogen centers. Alkyl groups offer the most direct means of implementing such changes. Perhaps the greatest impact from varying the organic groups would arise with changing the substituents on the third nitrogen atom where, depending on the size and the number of the alkyl groups, the plane formed by the NR'_2 or N(H)R' and the core NCN plane can range anywhere from 0 to 90° (Scheme 3). At or near zero this third nitrogen exerts an effect on NCN, which pushes the alkyl groups towards the metal and so increases the overall sterics of the system. At or near 90° the third nitrogen and its substituents are perpendicular to the ligand plane and relieves steric crowding about the metal while at the same time adding what can be effectively considered as bulk above and below the planar NCN moiety.

The electronic features that are unique to guanidinate ligands, compared to the carboxylate analogues, arise from the possibility of π delocalization of the NR'_2 or N(H)R' lone pair (II, Scheme 4). This would increase the charge on the nitrogen atoms bonded to the metal and lead to increased metal-ligand bond strength in the complex, especially in the case of high oxidation states or electron deficient metals. Furthermore, restriction of the R groups to alkyls removes the possibility of unanticipated resonance contributions and, through inductive effects, will likely increase the donor ability of the ligand. Of course such an interaction requires a planar third nitrogen and the 0° orientation of this group described above. Clearly the interplay of sterics and electronics will be important and interesting.

Several modes of coordination are available to guanidinate complexes (Scheme 4). Guanidines have been reported to function as neutral donors, through the imine nitrogen lone

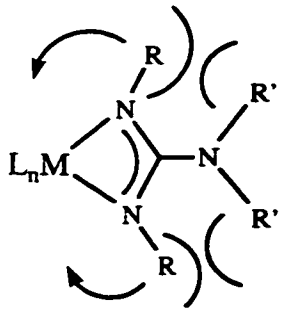

I (0°)

Increased steric interaction
overall a more bulky ligand

VS

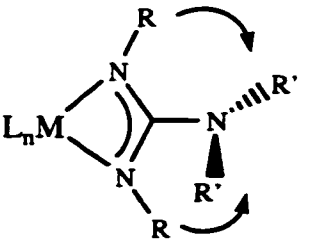

II (90°)

Removal of steric interaction
overall a less bulky ligand

Scheme 3

Monoanionic tri and tetrasubstituted

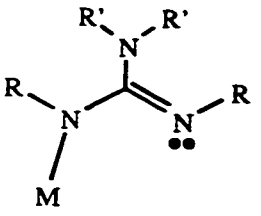

I

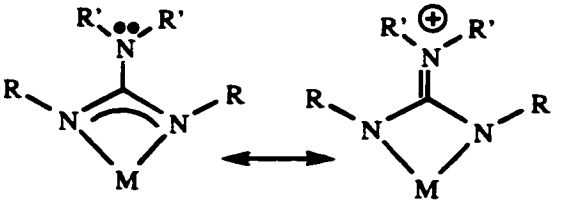

II

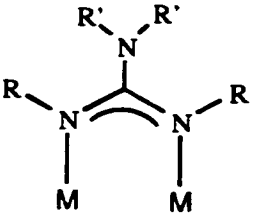

III

R' = alkyl or H

Dianionic trisubstituted

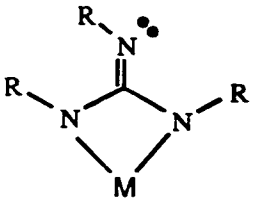

IV

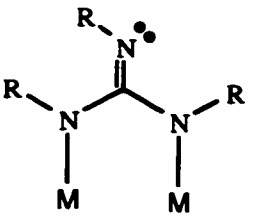

V

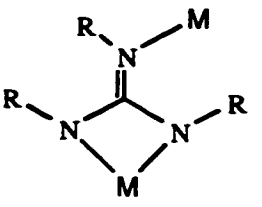

VI

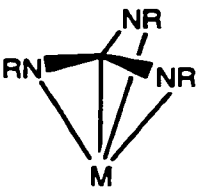

VII

Scheme 4

pair, to metal centers. This may be the largest area of guanidine research, however this mode is not in the scope of this thesis. Structures I, II, and III all display monoanionic guanidinate ligands coordinating in monodentate, chelating bidentate and bimetallic bidentate bonding modes respectively.

An important consideration in guanidine chemistry is the possible formation of a dianionic ligand. For example the N, N', N"-trisubstituted guanidinate ligand can be doubly deprotonated to yield a dianionic species. Such a compound is then isoelectronic with the trimethylenemethane dianion which is known to coordinate a wide range of metals in the η^4 mode, and might exhibit similar π delocalization involving the three pairs of p electrons on three sp^2 hybridized nitrogen centers. However, it is important to realize that in practice the TMM ligand does not appear to be a substitute for the cyclopentadienyl ligand. For example, initial studies have shown that iron TMM complexes are susceptible to electrophilic attack as evidenced by the addition of HCl to tris(carbonyl)-η^4-trimethylenemethaneiron to give chlorotris(carbonyl)-2-methylallyliron(II). As well some cationic TMM complexes are susceptible to nucleophilic attack at the trimethylenemethane ligand, forming neutral substituted η^3-allyl complexes. We hope that the guanidine dianion will be able to withstand these types of rearrangements and in doing so test the guanidine dianions ability to function as a Cp equivalent.

A trisubstituted dianionic guanidinate ligand opens up several unique coordination modes unavailable to the tetrasubstituted guanidines. Two modes of binding chelating IV and bimetallic bidentate V seem most likely. Two other possible binding modes for the dianion, VI (tridentate bimetallic) and VII (π bonded ligand), have not yet been observed.

Guanidines can be introduced to the metal center in several convenient ways. Insertion of carbodiimides into an M-N bond yields a coordinated guanidine (Equation 1). This method is limited to the availability of metal amido complexes and the desired carbodiimide.

The metathesis reaction is perhaps more general and versatile and depends on being able to generate a salt of the guanidine ligand. For example, attack of a mono lithium salt of a guanidine on a metal halide should yield a monoanionic guanidinate complex and the corresponding salt. Similarly a dilithium salt of a guanidine should yield a dianionic guanidinate complex (Equation 2).

Another general method to incorporate guanidine anions into the metal coordination sphere relies on elimination reactions. In this technique a basic ligand, within the metal coordination sphere, can react with an acidic hydrogen on a nitrogen atom of the guanidine. The most synthetically convenient ligands that can be eliminated when protonated are those that are volatile and so can be easily separated from the product complex. Examples of choice elimination reactions involve elimination of H_2 from metal hydrides, elimination of an alkane from a metal alkyl, and elimination of amine from a metal amido complex (Equation 3). In many cases, these reactions can also involve the loss of an additional neutral ligand (e.g. CO) in order to open a coordination site for the guanidinate ligand. Another possibility is the elimination of HX (X = halogen) from halo metal complexes. This procedure requires the use of a base to drive the reaction forward and since guanidine is a very strong base a guanidinium salt would likely be formed. This by-product may be difficult to separate from the desired product.

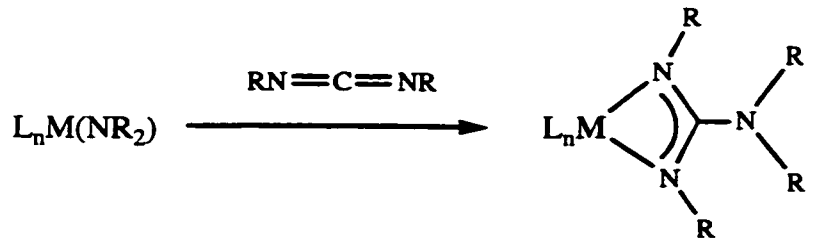
RN=C=NR
$L_nM(NR_2)$
L_nM

(1)

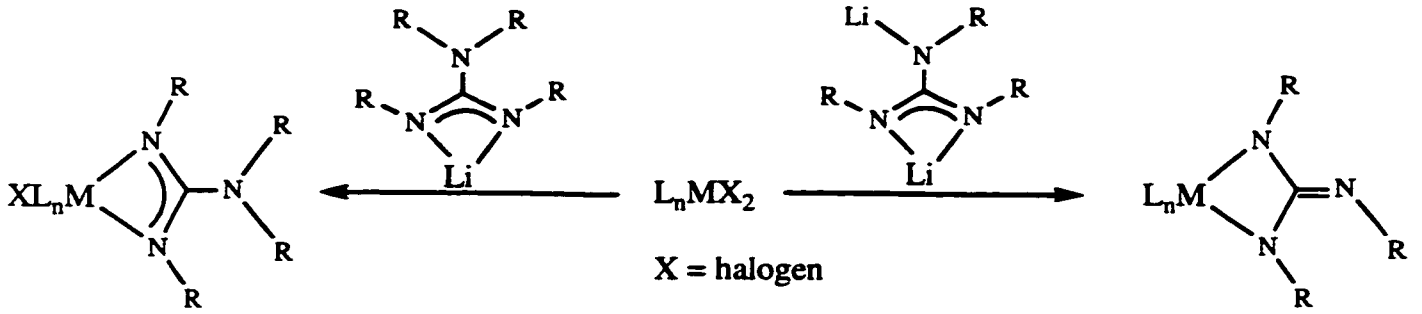
XL_nM
Li
L_nMX_2
X = halogen
Li
L_nM

(2)

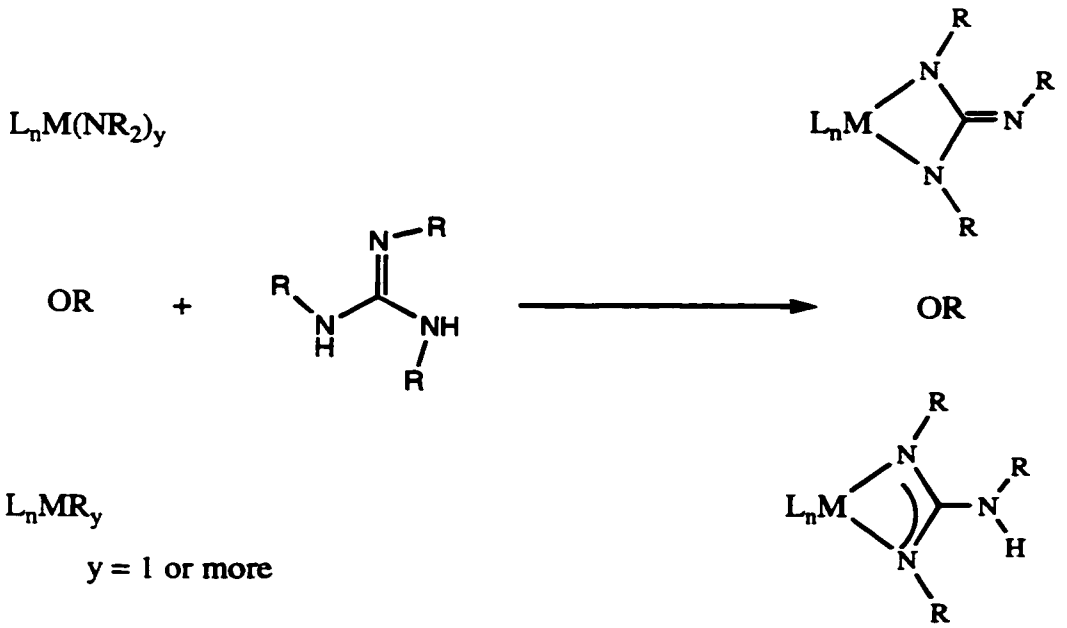
$L_nM(NR_2)_y$
OR
+
OR
L_nMR_y
y = 1 or more
L_nM
L_nM

(3)

Literature Review

The following review is organized by groups of metals and not by the types of reactions they undergo with guanidines. The review is restricted to all transition metal guanidinate complexes that are of the tri and tetra alkyl substituted guanidine variety. Other possibilities are not in the scope of this thesis and are not shown. Reactions are presented in schemes, which are designed to show some general methods for introduction of guanidines to the metal coordination sphere. Several unique products are shown to give a visual impression of the modes of bonding that have been observed for guanidines. Neutral coordination of guanidines is not in the scope of this thesis and is not discussed in this review.

Group 4 (Ti, Zr, Hf)

Reaction with $M(NMe_2)_4$ (M = Ti) with di(p-tolyl)carbodiimide and (M = Ti, Zr, Hf) with dicyclohexylcarbodiimide gave the tetrasubstituted guanidinate complexes in good yield (Equation 4).[1] Further insertions of carbodiimide were prevented due to steric congestion. No attempts were made to prepare the mono insertion product.

A proposed mechanism for leading to the bidentate guanidinate anion involves a 1, 2 insertion of the C=N bond into the negatively polarized amido ligand followed by the coordination of the imine lone pair to the metal center (Scheme 5).

Group 5 (V, Nb, Ta)

$M(NMe_2)_5$ (M = Ta, Nb) complexes react with carbodiimides to provide $[(RN)_2CNMe_2]M(NMe_2)_4$ (R = ^{i}Pr, Cy) (Equation 5).[2] Spectroscopic methods, elemental analysis and single crystal x-ray diffraction studies have characterized these new guanidinate

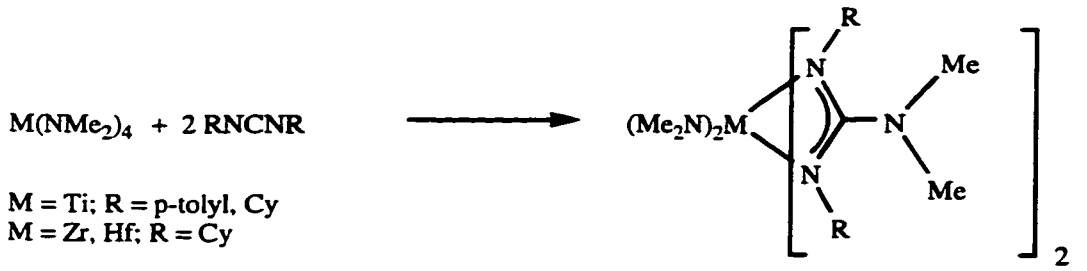

(4)

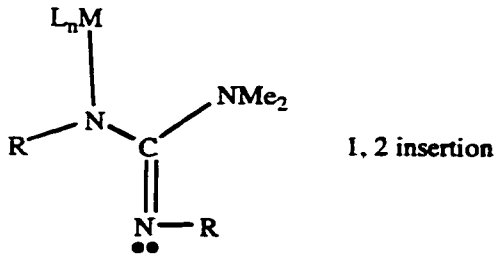

1, 2 insertion

Scheme 5

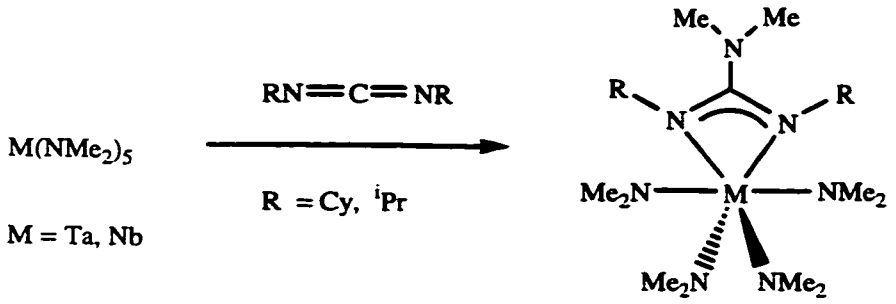

(5)

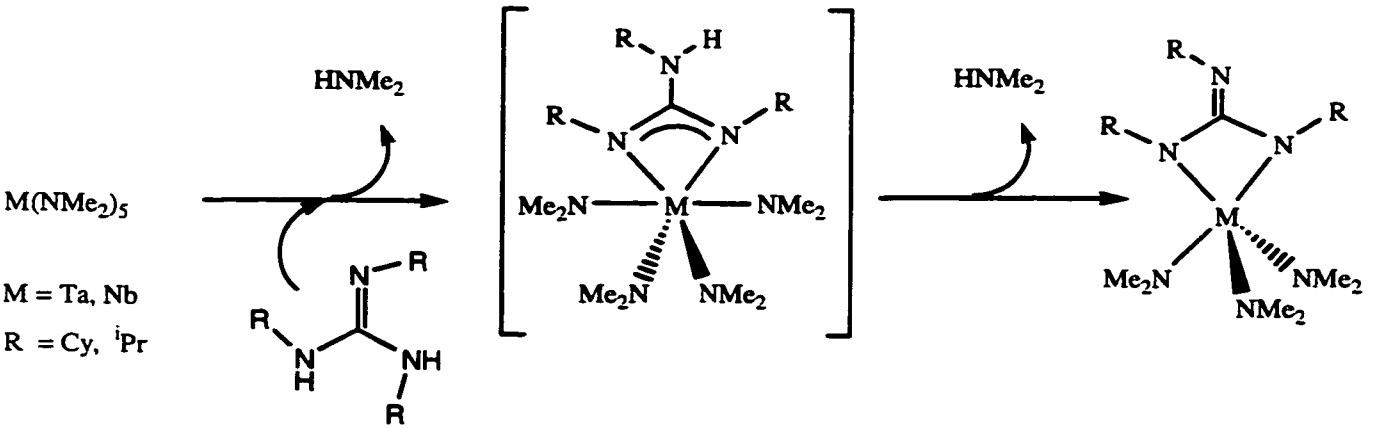

(6)

complexes. Incorporation of a second equivalent of carbodiimide was unsuccessful possibly due to increased steric congestion after a single insertion. $M(NMe_2)_5$ (M = Ta, Nb) also reacts with N, N', N"-trialkylguanidine (alkyl = ^{i}Pr, Cy) to yield a series of dianionic guanidinate complexes with the formula, $[(RN)_3C]M(NMe_2)_3$.[3] By taking advantage of the acidic protons on the guanidine a deprotonation reaction occurs involving the basic amido ligands and forming free amine as the by-product. Spectroscopic as well as crystallographic studies confirmed the identity of these compounds and suggest that these reactions proceeded directly to dianionic guanidinate complexes (Equation 6). Attempts to introduce another equivalent of guanidine were unsuccessful, probably due to increased steric congestion. Analysis of the crystallographic data indicated that the negative charges are localized on the nitrogens bound to the metal.

Also reported is the isolation of a related species $TaCl(NMe_2)_3[(^iPrN)_2C(NH^iPr)]$ containing a monoanionic ligand formed by reaction of $Ta(NMe_2)_4Cl$ and triisopropyl guanidine. This complex can be transformed to the species containing a dianionic ligand and three amido groups by addition of $LiNMe_2$.[4]

Group 6 (Cr, Mo, W)

The dinuclear complex $Mo_2\{\mu\text{-}[(PhN)_2C(NHPh)]_4\}$[5] containing four bridging triphenylguanidinate monoanions was prepared by the reaction of $Mo(CO)_6$ with triphenylguanidine through a combination substitution/redox reaction generating H_2 and Mo(II) (Equation 7). This complex could be reversibly oxidized by both one and two electrons using $AgBF_4$ and $[NH_4]_2[Ce(NO_3)_6]$ respectively. An x-ray crystal structure of the parent and mono-cationic complexes indicated the angle between the NCN plane and the N(H)Ph plane was to large for any significant π overlap to be present.

$CpMo(CO)_3Cl$ reacted with triphenyl guanidine, eliminating HCl as the guanidinium hydrochloric salt, to form $CpMo(CO)_2[(PhN)_2C(NHPh)]$.[6] A crystal structure of this molybdenum compound revealed the symmetrical chelating coordination of the guanidinate ligand (Equation 8).

Group 7 (Mn, Tc, Re)

Only at higher temperatures and in the presence of excess triphenylguanidine does Br^- in $MnBr(CO)_5$ react with the guanidine to eliminate HBr and produce a monoanionic bound guanidine $Mn[(PhN)_2C(NHPh)](CO)_4$. In this case the mode of coordination was assumed to be bidentate and anionic.[6]

Group 8 (Fe, Ru, Os)

Syntheses of the tricyclohexylguanidine[7] and triisopropylguanidine[8] dianions coordinated to a dinuclear iron hexacarbonyl framework have been reported. These compounds were isolated as the unanticipated product of the reaction of $Fe(CO)_5$ and carbodiimide. The crystal structure of the cyclohexyl complex was determined (Scheme 6).

The chloro-bridged dimer $[(\eta^5\text{-}MeC_6H_4{}^iPr\text{-}p)RuCl_2]_2$ reacts with 4 equivalents of triphenylguanidine yielding the air stable $[Ru(\eta^5\text{-}MeC_6H_4{}^iPr\text{-}p)\{(NPh)_2C(NHPh)\}Cl]$[9] complex as well as 2 equivalents of the HCl guanidine $(NHPh)_3CCl$. This species was the first example of a structurally characterized monomeric complex with a chelating guanidinate monoanion. Proton NMR spectra indicated a 2:1 ratio for the phenyl groups of the triphenylguandinate ligand consistent with free rotation about the C-N bond in the C(NHPh) moeity.

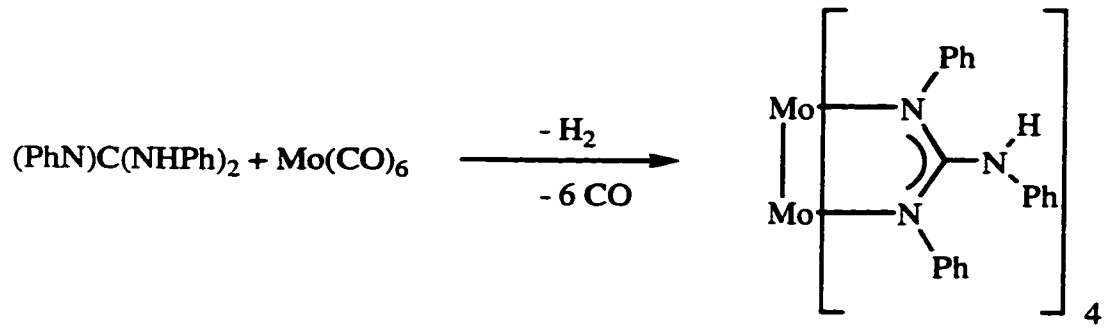

(7)

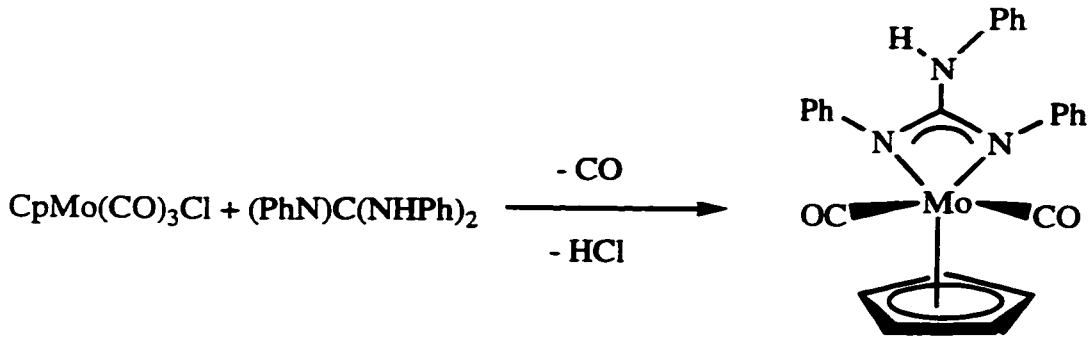

(8)

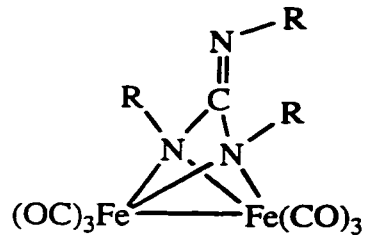

R = Cy, ^{i}Pr

Scheme 6

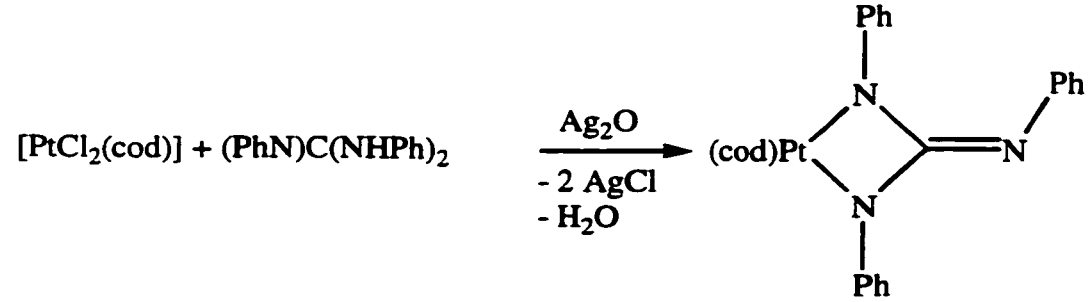

(9)

Group 9 (Co, Rh, Ir)

The chloro-bridged dimer $[(\eta^5\text{-}C_5Me_5)RhCl_2]_2$ reacts with 4 equivalents of triphenylguanidine yielding the air stable complex $ClRh(\eta^5\text{-}C_5Me_5)[(NPh)_2C(NHPh)]$[9] and 2 molar equivalents of HCl guanidine $(NHPh)_3CCl$. This compound was structurally and spectroscopically analyzed and showed a 2:1 proton NMR ratio for the phenyl groups.

Group 10 (Ni, Pd, Pt)

One of the very few examples of a guanidine dianion coordinated to a transition metal center is the reaction of $PtCl_2(cod)$ with one equivalent of triphenylguanidine in the presence of excess silver(I)oxide. Work up gave an air-stable crystalline solid of $(cod)Pt[(NPh)_3C]$[10] in 94% yield (Equation 9). The crystal structure shows the presence of a localized double bond and it is suggested that the orientation of the imino phenyl precludes the fully symmetrical binding of the ligand to the platinum metal.

Thesis Goals and Approaches

This thesis focuses on guanidinates with a high degree of substitution, i.e. tri, and tetra alkyl substituted guanidines. The literature on this type of guanidine is quite scarce and not very well developed. The few reported results with these ligands provide some ideas on methods for introduction of guanidine ligands into the coordination sphere of a metal, but little regarding the principles for predicting bonding modes and essentially nothing regarding the reactivity of such complexes.

As this thesis work began, the central objective was the synthesis of early transition metal guanidinate complexes with the goal of exploring the issues involved in metal-ligand

bonding. This required the development of fundamental ideas regarding the introduction of guanidinate anions and dianions to the metal center, the features that favor different binding modes of the ligand, and the general reactivity characteristics of these complexes. To accomplish these goals the sterics, electronics, and ultimately the structural properties imparted by these ligands were investigated. Steric investigation began by synthesizing two tetra substituted guanidinate ligands and one tri substituted ligand. Then with these ligands in hand a variety of complexes were synthesized and their structural properties investigated. In addition to changing the number of substituents, the types of substituent groups were varied. Specifically, isopropyl groups replaced the bulky trimethylsilyl substituents. It was anticipated that alkyl groups might also be used to investigate the electronic component of the system, as alkyl groups would be more electron releasing. This might make the alkyl ligand a more powerful electron donor compared to the trimethylsilyl counterpart. Moreover, employing these ligands in complexes of groups 4 and 5 certainly opened up new steric and electronic considerations. Finally, the development of new ideas on how guanidinate ligands can be introduced to the metal was investigated.

Guanidinate anions have several unique characteristics that form the basis of the work found in this thesis. These features are all coupled to the presence of a third nitrogen site within the ligand and to analyze and characterize the new guanidinate complexes found in this thesis, standard techniques such as ^{1}H and ^{13}C NMR, and EA were used. However, to fully investigate the bonding characteristics of the metal-ligand interactions a significant amount of single crystal x-ray diffraction studies were performed. This study in particular can answer the question of whether the lone pair of the uncoordinated nitrogen is located on this nitrogen or delocalized within the ligand (II, Scheme 4). Data such as C-N bond length comparisons combined with calculated dihedral angles can help determine the degree to

which full π delocalization has occurred in the guanidinate ligand. In conjunction with this data, the range of complexes synthesized in this thesis may allow understanding of the influence of supporting ligands bound to the metal on the guanidine binding characteristics, especially the factors involved in monoanionic *vs* dianionic guanidinate formation.

References

(1) Chandra, G.; Jenkins, A. D.; Lappert, M. F.; Srivastava, R. C. *J. Chem. Soc. (A)* **1970**, 2550

(2) Tin M.K.T.; Yap G. P. A.; Richeson D. S. *Inorg. Chem.* **1999**, 38, 998

(3) Tin M.K.T.; Yap G. P. A.; Richeson D. S. *Inorg. Chem.* **1998**, 37, 6728

(4) Tin M.K.T.; Thirupathi N.; Yap G. P. A.; Richeson D. S. *J. Chem. Soc., Dalton Trans.* **1999**, 2947

(5) Bailey, P. J.; Bone, S. F.; Mitchell, L. A.; Parsons, S.; Taylor, K. J.; Yellowless, L. *Inorg. Chem.* **1997**, *36*, 867

(6) da S. Maia, J. R.; Gazard, P. A.; Kilner, M. Batsanov, A. S.; Howard, J. A. K. *J. Chem. Soc., Dalton Trans.* **1997**, 4625

(7) Bremer, N. J.; Cutcliffe, A. B.; Farona, M. F. *J. Chem. Soc., Chem. Commun.* **1970**, 932

(8) Bremer, N. J.; Cutcliffe, A. B.; Farona, M. F.; Kofron, W. G. *J. Chem. Soc. (A)* **1971**, 3264

(9) Bailey, P. J.; Mitchell, L. A.; Parsons, S. *J. Chem. Soc., Dalton Trans.* **1996**, 2839

(10) Dinger, M. B.; Henderson, W. *Chem. Commun.* **1996**, 211

Chapter 2

N-Substituted Guanidinate Anions as Ancillary Ligands in Group 4 Chemistry

Introduction

As discussed in the introduction one of the ways to introduce a guanidinate ligand into the coordination sphere of a metal center is by using a lithium salt of the guanidine and a metal chloride. In this chapter lithium guanidinate anions were generated by the direct reaction of either 1,3-dicyclohexylcarbodiimide or 1,3-diisopropylcarbodiimide (RN=C=NR; R = Cy, ^{i}Pr) with one equivalent of $LiN(SiMe_3)_2$ in diethyl ether.

A key feature of guanidinate ligands is the presence of the NR'_2 function, which allows consideration of a zwitterionic resonance structure (**I**) (Scheme 1). If this contribution is important it should lead to more polarized M-N bonds and electrophilic metal centers. Of course, for this contribution to be significant the NR'_2 center must be planar, sp^2 hybridized with the lone pair residing in a p-orbital which would then be available for overlap with the conjugated NCN moiety and there must be a small dihedral angle between the planes defined by the CNR'_2 groups and that defined by NCN in order for substantial overlap to occur. Keeping in mind these two requirements, it is interesting to note that the attendant steric congestion caused by the two bulky organic substituents on the third nitrogen would probably encourage a larger dihedral angle thus discouraging the appropriate orientation for π conjugation.

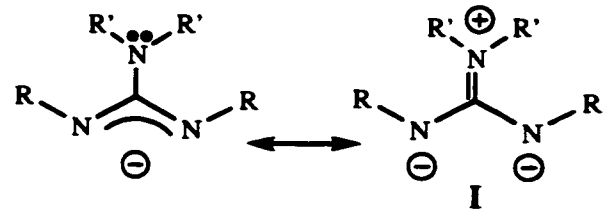

I

Scheme 1

Experimental

General Considerations

All manipulations were carried out in either a nitrogen filled drybox or under nitrogen using standard Schlenk-line techniques. $LiN(SiMe_3)_2$, CyNCNCy, $^iPrNCN^iPr$, $ZrCl_4$, and $HfCl_4$ were used as received from Aldrich Chemical Company. Solvents were distilled under nitrogen from Na/K alloy. $ZrCl_4(THF)_2$ and $HfCl_4(THF)_2$ were prepared by literature procedures. Deuterated benzene was purified by vacuum transfer from potassium metal. ^1H and ^{13}C NMR spectra were run on a Gemini 200 MHz spectrometer with deuterated benzene or pyridine as a solvent and internal standard. All elemental analyses were run on a Perkin Elmer PE CHN 4000 elemental analysis system.

Li{CyNC[N(SiMe$_3$)$_2$]NCy}

Addition of a solution of $LiN(SiMe_3)_2$ (2.239 g, 13.4 mmol) in 30-ml diethylether to CyNCNCy (2.761 g, 13.4 mmol) in 30-ml diethylether gave a clear pale yellow solution. The reaction mixture was allowed to stir for four hours. The solvent was removed under vacuum to give a white powder (4.64 g, 93% yield). ^1H NMR (C_6D_6, ppm) 3.38 (br, C_6H_{11}, 2H), 1.95-1.05 (br, C_6H_{11}, 20H), 0.33 (s, CH_3, 18H). ^{13}C NMR (C_6D_6, ppm) 163.90 (s, N_3C), 54.29, 38.70, 26.62, 26.13 (4s, C_6H_{11}), 2.63 (s, CH_3)

Li{^{i}PrNC[N(SiMe$_3$)$_2$]N^{i}Pr}

Addition of a solution of $LiN(SiMe_3)_2$ (2.850 g, 17.0 mmol) in 30-ml diethylether to $^iPrNCN^iPr$ (2.150 g, 17.0 mmol) in 20-ml diethylether gave a clear pale yellow solution. The mixture was allowed to stir for four hours. The solvent was removed under vacuum to give a

very light peach colored solid (4.34 g, 87% yield). ^{1}H NMR (C_6D_6, ppm) 3.72 (sept., CH, 2H), 1.12 (d, CH_3, 12H), 0.31 (s, CH_3, 18H). ^{13}C NMR (C_6D_6, ppm) 163.95 (s, N_3C), 45.70, 27.71 (2s, $CH(CH_3)_2$), 2.56 (s, CH_3)

$Zr[^iPrNC[N(SiMe_3)_2]N^iPr]_2Cl_2$ (1)

A reaction flask was charged with $ZrCl_4(THF)_2$ (0.568 g, 1.51 mmol), 50-ml diethylether and a stir bar. To this was added $Li[^iPrNC(SiMe_3)_2N^iPr]$ (0.906 g, 3.09 mmol). After allowing the reaction mixture to stir for 16 hours the mixture was filtered and the solvent was evaporated from the clear yellow filtrate under vacuum to give pale yellow powder (0.464 g, 42%). Colorless crystals obtained from toluene at -34 °C. ^{1}H NMR (C_6D_6, ppm) 3.93 (sept., CH, 4H), 1.48 (d, CH_3, 24H), 0.25 (s, CH_3, 36H). ^{13}C NMR (C_6D_6, ppm) 175.23 (s, N_3C) 47.33 (s, $CH(CH_3)_2$), 25.47 (s, $CH(CH_3)_2$), 2.90 (s, $SiCH_3$). Anal. Calcd for $ZrCl_2Si_4N_6C_{26}H_{64}$: C 42.47, H 8.77, N 11.43. Found: C 42.94, H 8.90, N 10.86.

$Hf[^iPrNC[N(SiMe_3)_2]N^iPr]_2Cl_2$ (2)

Following an experimental procedure similar to **1** using $HfCl_4(THF)_2$ (1.129 g, 2.43 mmol) and $Li[^iPrNC(SiMe_3)_2N^iPr]$ (1.463 g, 4.98 mmol) in diethylether gave an off white powder (1.399 g, 70% yield). Colorless crystals obtained from toluene at -34 °C. ^{1}H NMR (C_6D_6, ppm) 4.11 (sept, CH, 4H), 1.48 (d, CH, 24H), 0.25 (s, CH_3, 36H). ^{13}C NMR (C_6D_6, ppm) 174.69 (s, N_3C) 47.02 (s, CH), 25.48 (s, CH_3). 2.93 (s, Si-CH_3). Anal. Calcd for $HfCl_2Si_4N_6C_{26}H_{64}$: C 37.96, H 7.84, N 10.22. Found: C 37.60, H 7.80, N 9.77

$Zr[CyNC(SiMe_3)_2NCy]_2Cl_2$ (3)

Following a similar experimental procedure as for **1** using $ZrCl_4(THF)_2$ (0.421 g, 1.1 mmol) and $Li[CyNC(SiMe_3)_2NCy]$ (0.855 g, 2.3 mmol) gave a very light yellow solid (0.72 g, 73% yield). Colorless crystals obtained from toluene at –34 °C. ^1H NMR (C_6D_6, ppm) 3.50 (br, C_6H_{11}, 4H), 1.0-2.2 (br, C_6H_{11}, 40H), 0.3 (s, CH_3, 36H). ^{13}C NMR (C_6D_6, ppm) 175.17 (s, N_3C) 56.08, 35.36, 35.17, 26.34 (4s, C_6H_{11}), 3.12 (s, Si-CH_3).

$Hf[CyNC(SiMe_3)_2NCy]_2Cl_2$ (4)

Following an experimental procedure similar to **1** using $HfCl_4(THF)_2$ (1.418 g, 3.1 mmol) and $Li[CyNC(SiMe_3)_2NCy]$ (2.338 g, 6.3 mmol) gave a white powder (2.54 g, 83% yield). Colorless crystals obtained from toluene at -34 °C. ^1H NMR (C_6D_6, ppm) 3.68 (br, C_6H_{11}, 4H), 1.90-1.20 (br, C_6H_{11}, 40H), 0.32 (s, CH_3, 36H). ^{13}C NMR (C_6D_6, ppm) 174.61 (s, N_3C), 55.66, 35.03, 26.26, 25.61 (4s, C_6H_{11}), 3.17 (s, Si-CH_3). Anal. Calcd for $C_{38}H_{80}N_6Si_4HfCl_2$: C 46.44, H 8.20, N 8.55. Found: C 46.18, H 8.31, N 8.36

$Zr\{[CyNC(SiMe_3)_2NCy]Cl_4\}Li(THF)_2[Et_2O]$ (5)

A reaction flask was charged with $ZrCl_4(THF)_2$ (1.333 g, 3.5 mmol), 50-ml diethylether and a stir bar. To this was added $Li[CyNC(SiMe_3)_2NCy]$ (1.320 g, 3.5 mmol). After stirring for 20 hours the reaction mixture was filtered through celite to give a clear pale lemon yellow filtrate. The solvent was then removed under vacuum to give a very light green powder (1.96 g, 68% yield). Pale-yellow crystals were obtained from diethylether at –34 °C. ^1H NMR (py-d_5, ppm) 3.75 (br m, C_6H_{11}, 2H), 3.60 (m, THF, 8H), 3.31(q, Et_2O, 4H) 2.68-1.26 (br, C_6H_{11}, 20H), 1.61 (m, THF, 8H), 1.12 (t, Et_2O, 6H), 0.43 (s, CH_3, 18H). ^{13}C NMR

(py-d_5, ppm) 171.93 (s, N_3C), 67.77, 25.41 (2s, THF), 65.72, 15.46 (2s, diethylether), 55.76, 34.89, 25.99, 25.77 (4s, C_6H_{11}), 2.56 (s, CH_3).

$Hf\{[CyNC(N(SiMe_3)_2)NCy]Cl_4\}\{Li(THF)_3\}$ (6)

Using an experimental procedure similar to **5** the reaction of $HfCl_4(THF)_2$ (0.713 g, 1.5 mmol) and $Li[CyNC(SiMe_3)_2NCy]$ (0.573 g, 1.5 mmol) gave a colorless filtrate. The solvent was then removed under vacuum to give a white powder (0.908 g, 66% yield). Colorless crystals were obtained from diethylether at –34 °C. ^1H NMR (py-d_5, ppm) 3.75 (br, C_6H_{11}, 2H), 3.62 (m, THF, 12H), 2.68-1.25 (br, C_6H_{11}, 20H), 1.59 (m, THF, 12H), 0.43 (s, CH_3, 18H). ^{13}C NMR (py-d_5, ppm) 170.29 (s, N_3C), 67.81, 25.79 (2s, THF), 55.43, 35.05, 26.43, 26.06 (4s, C_6H_{11}), 2.64 (s, CH_3).

$[CyNC(SiMe_3)_2NCy]ZrBz_3$ (7)

In a reaction flask compound **5** (1.000 g, 1.21 mmol) was dissolved in 10-ml of toluene. To the stirring solution, BzMgCl (4.5-ml, 1.0 M in diethylether) was added dropwise and the reaction mixture was allowed to stir for 2 hours. Removal of solvent followed by extraction of the resultant solid with 10-ml toluene, filtration, concentration and cooling to -34 °C gave orange crystals (0.64 g, 72 %). ^1H NMR(C_6D_6, ppm) 7.22-6.91 (m, C_6H_5, 15H), 3.50 (br, CH, 2H), 2.50 (s, CH_2, 6H), 1.75-0.88 (br, C_6H_{11}, 20H), 0.18 (s, CH_3, 9H). ^{13}C NMR (C_6D_6, ppm): 174.19 (s, N_3C), 144.75 (s, C_6H_5), 129.43, 128.22, 122.83 (3s, C_6H_5), 77.36 (s, CH_2), 56.38 (s, CH), 35.07, 26.45, 25.68 (3s, C_6H_{11}), 2.36 (s, CH_3).

Results and Discussion

Lithium guanidinate salts are easily generated by the reaction of carbodiimide with the appropriate amido species. The lithium guanidinate salts could be isolated in pure form by simple removal of the solvent. However, in most cases metathesis reactions with Zr and Hf chlorides can be carried out with freshly prepared solutions of lithium guanidinate. Depending on the metal:ligand ratio used in the reaction a series of bis(guanidinate) and mono(guanidinate) complexes of Zr and Hf exhibiting the general formula $\{RNC[N(SiMe_3)_2]NR\}_2MCl_2$ (R = isopropyl, M = Zr **1**, Hf **2**; R = cyclohexyl, M = Zr **3**, Hf **4**) and $\{CyNC[N(SiMe_3)_2]NCy\}MCl_4]^-$ (M = Zr **5**, Hf **6**) were isolated. Complex **5** provides an access to the organometallic derivative $\{CyNC[N(SiMe_3)_2]NCy\}ZrBz_3$ **7** by reaction with 3 equivalents of BzMgCl (Scheme 2). These results provide the first reported example of an organo-zirconium complex supported by a guanidinate ligand.

Bis(guanidinate) Complexes of Zr and Hf

Spectroscopic characterization provided the first confirmation of the identity of these materials. Specifically, compounds **1-4** exhibited similar ^1H and ^{13}C NMR spectra with the most notable features being: (1) the appearance of single isopropyl or cyclohexyl substituents as indicated by single proton and carbon resonances for the NCH groups, and (2) appearance of one resonance for the $SiMe_3$ moieties of the NR'_2 groups. On the basis of the NMR observations and the results of the crystallographic characterization described below for **1, 3** and **4** we propose the C_2 symmetric structures for these complexes shown in Scheme 2. The fact that the two ends of the guanidinate ligand appear to be equivalent on the NMR time scale is consistent with compounds **1-4** being fluxional.

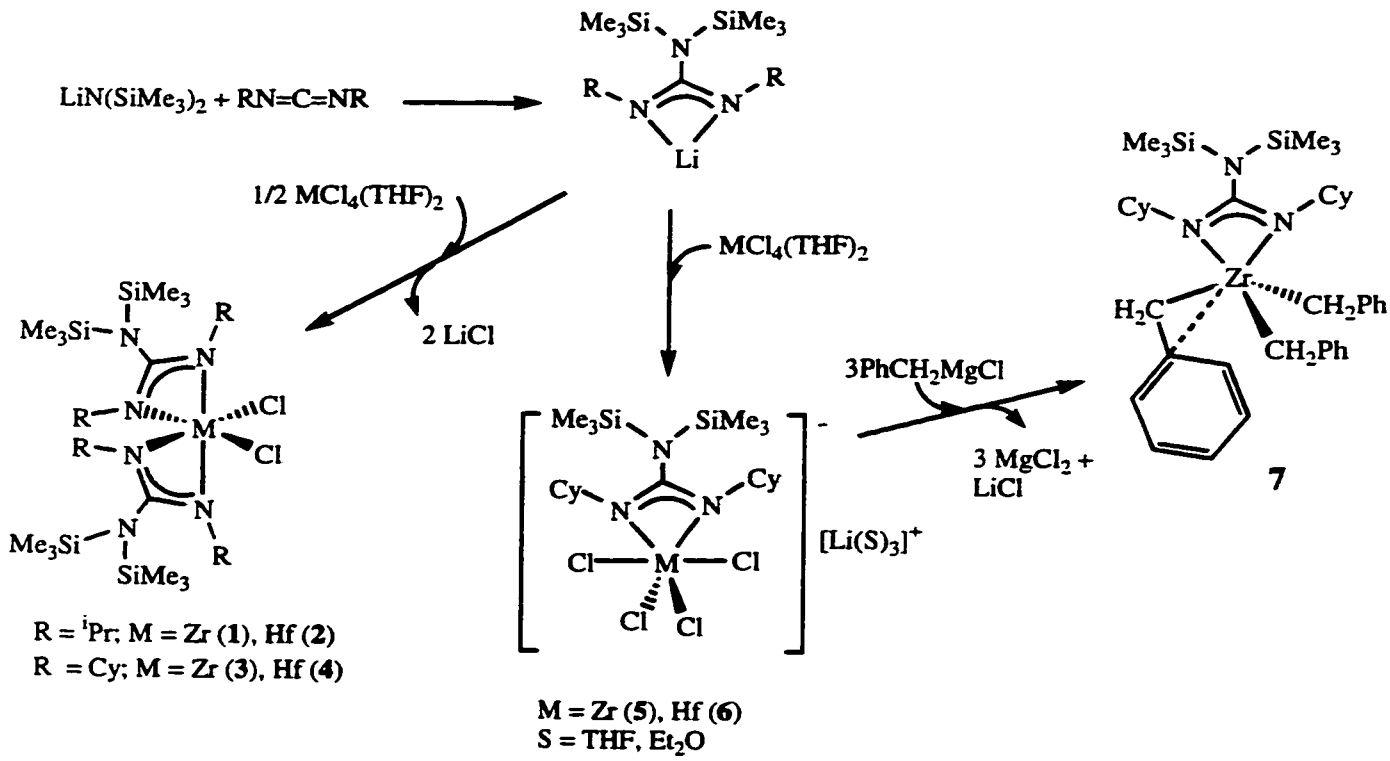

Scheme 2

Single crystal x-ray diffraction analyses of **1**, **3** and **4** were undertaken in order to establish the coordination geometry of the metal center, and the connectivity of the ligand for these compounds (Table 1). The results of these structural studies are displayed in Figures 1, 2 and 3 and summarized in Tables 2-4.

In all three cases, the metal center is in a distorted pseudooctahedral environment consisting of the four nitrogen atoms of two bidentate guanidinate anions with cis-chloride ligands completing the coordination sphere. Table 2 presents a summary of selected bond distances and angles for **1**. This complex possesses a crystallographic C_2 axis bisecting the Cl-Zr-Cl(A) axis which makes the two guanidinate ligands equivalent. The two nitrogens N(1), N(2) and bridging carbon atom C(7) for the guanidinate lie in a plane which includes the Zr atom. The termini of the guanidinate ligand can be divided into two types, the cis-

N^{i}Pr groups N(1), N(1A) with a N-Zr-N angle of 98.1(2)° and trans-N^{i}Pr groups N(2), N(2A) with a N-Zr-N angle of 164.9(2)°. The structural features of **1** are quite similar to the amidinate complex $[CyNC(Me)NCy]_2ZrCl_2$ which was recently reported[1]. Of particular interest when analyzing the steric requirements of these ligands is a comparison of the angles around the N atoms in **1** and in $[CyNC(Me)NCy]_2ZrCl_2$ (Chart 1). It is noteworthy that the C(bridge)-N-R (R = Cy, ^{i}Pr) angle and the Zr-N-R angle for these two species are comparable indicating that although the substituent on the methyne carbon is larger in **1** ($N(SiMe_3)_2$ vs. Me), the effective steric effects within the ligand framework are nearly the same.

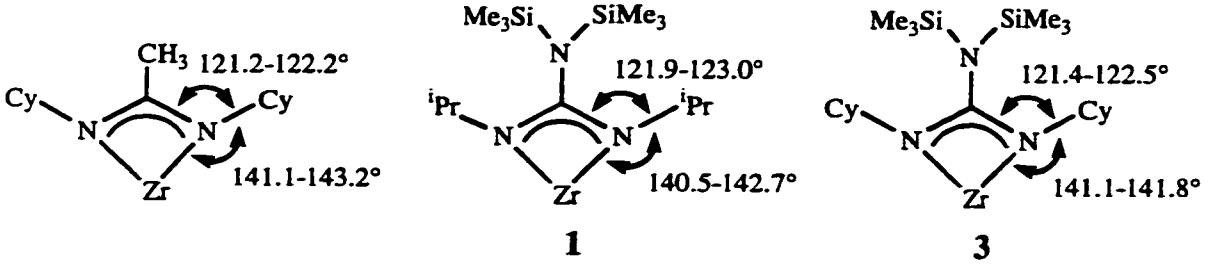

1 **3**

Chart 1

An alternative description of the Zr coordination geometry of **1** is as a distorted pseudotetrahedral complex with the vectors that bisect the guanidinate ligands, Zr-C(7) and Zr-C(7A), defining two of the vertices and the two Zr-Cl vectors defining the other two. This description emphasizes the relationship of **1-4** to metallocene dichloride systems and allows some comparison of the structural features between these species. For example the C(7)-Zr-C(7A) angle in **1** of 131.6(2)° is very similar to the Cp(centroid)-Zr-Cp(centroid) angle of 134° found in Cp_2ZrCl_2.[2] The observation that the Zr-Cl distances (2.420(2)Å) and Cl-Zr-Cl angle (90.23(12)°) are both smaller than the corresponding values found for Cp_2ZrCl_2 (2.44 Å and 97.1°) may reflect a higher degree of polarity in **1** compared to zirconocene dichloride.

Monomeric complexes **3** and **4** crystallize with the molecular geometries shown in Figures 2 and 3. These compounds exhibited geometric and structural features similar to that of **1**. In both cases, the metal centers lie on an approximate two-fold axis which bisects the Cl(1)-M-Cl(2) angle (M = Zr = 94.06(3)° M = Hf = 93.81(7)°) with two planar bidentate guanidinate anions. Tables 3 and 4 present a summary of selected bond distances and angles for complexes **3** and **4** respectively. As with **1**, the termini of the planar guanidinate ligands in these complexes can be divided into cis-NCy groups and trans-NCy groups. Again, an alternative pseudotetrahedral description based on the Zr-Cl(1), Zr-Cl(2), Zr-C(13), and Zr-C(32) vectors in **3** and the Hf-Cl(1), Hf-Cl(2), Hf-C(7), and Hf-C(26) vectors in **4** also provides satisfactory descriptions.

The dihedral angle formed by the planar $N(SiMe_3)_2$ function and the MNCN plane offers a means of evaluating the possibility of π-overlap between these two moieties. In the case of **1** an angle of 88.2(4)° is formed between these two planes while for **3** and **4** average dihedral angles of 86.3° and 85.8° were observed for the two crystallographically unique guanidinate ligands in each of these two complexes. This nearly perpendicular disposition is likely the result of steric interactions between the isopropyl or cyclohexyl functions and the bulky trimethylsilyl groups and eliminates significant π conjugation in both **1** and **4**. As a result structure **I** (Scheme 2) does not appear to be a significant contributor in these cases. However, this orientation of the bulky $N(SiMe_3)_2$ group effectively adds a third dimension to the steric bulk of what would be an otherwise planar guanidinate ligand. This perpendicular orientation also explains the observation that the guanidinate ligand in **1** appears to exhibit similar bonding parameters as the amidinate anion in $[CyNC(Me)NCy]_2ZrCl_2$ (Chart 1).[1]

Mono(guanidinate) complexes

A single tetrasubstituted guanidinate ligand can be introduced into the metal coordination sphere through reaction of a 1:1 ratio of lithium salt of N, N'-dicylohexyl-N"-bis(trimethylsilyl)guanidinate with either Zr or Hf chlorides. After crystallization from diethyl ether or THF, the new "ate" complexes $\{CyNC[N(SiMe_3)_2]NCy\}MCl_4]Li(S)_x$ (Scheme 2) (S = THF or THF/Et_2O) were isolated. The first indication that solvated Li cations remained in these materials was the appearance of coordinated solvent peaks in the NMR spectra of **5** and **6**. These spectra also display the characteristic signals for the guanidinate ligand.

The proposed structures for **5** and **6** (Scheme 2) were confirmed by x-ray crystallographic characterization, which yielded the results summarized in Figures 4 and 5 and Tables 5, 6 and 7.

In both cases the anionic complexes possessed a single bidentate guanidinate and four chloro ligands giving a distorted octahedral coordination geometry. The guanidinate ligands occupy two of the octahedral sites and exhibit bonding parameters that are similar to each other and to the bis(guanidinate) complexes **1**, **3** and **4**. The coordination geometry of these two complexes can also be reasonably described as pseudotrigonal bipyramidal with the central C of the guanidinate ligand and cis-chloro ligands forming the equatorial plane C(13), Cl(2) and Cl(3) for **5** and C(13), Cl(1), Cl(2) for **6**). The dihedral angles formed between the two planes defined by the $N(SiMe_3)_2$ function and the MNCN cycle again indicate little π-bonding interaction between these moieties (85.8(7)° for **5** and 86.0(9)° for **6**).

Table 1. Crystal data for compounds $\{^{i}PrNC[N(SiMe_3)_2]N^{i}Pr\}_2ZrCl_2$ **(1)**, $\{CyNC[N(SiMe_3)_2]NCy\}_2ZrCl_2$ **(3)**, and $\{CyNC[N(SiMe_3)_2]NCy\}_2HfCl_2$ **(4)**.

Empirical formula	$C_{26}H_{64}Cl_2N_6Si_4Zr$ (1)	$C_{38}H_{80}Cl_2N_6Si_4Zr$ (toluene) (3)	$C_{38}H_{80}Cl_2HfN_6Si_4$ $(benzene)_{0.5}$ (4)
Formula weight	735.31	987.69	1018.76
Temperature (K)	203(2)	203(2)	213(2)
Wavelength (Å)	0.71073	0.71073	0.71073
Crystal system	Orthorhombic	Monoclinic	Monoclinic
Space group	Pbcn	$P2_1/c$	$P2_1/c$
Unit cell dimensions (Å, deg)	a = 12.5453(17)	a=13.818(3)	a = 13.7878(6)
	b = 17.701(2)	b=18.534(4)	b = 18.5571(9)
	c = 18.012(2)	c=21.369(4)	c = 21.4427(10)
	$\alpha = 90$	$\alpha=90$	$\alpha = 90$
	$\beta = 90$	$\beta=92.716(4)$	$\beta = 92.8210(10)$
	$\gamma = 90$	$\gamma=90$	$\gamma = 90$
Volume ($Å^3$), Z	3999.9(9), 4	5466(2), 4	5479.7(4), 4
Density (Mg/m^3) (calculated)	1.221	1.200	1.235
Absorption coefficient (mm^{-1})	0.552	0.421	2.119
F(000)	1568	2120	2125
Crystal size (mm)	0.1 x 0.1 x 0.1	0.20x0.20x0.10	0.20 x 0.10 x 0.10
Limiting indices	$0 \le h \le 16$	$-18 \le h \le 18$	$-18 \le h \le 16$
	$0 \le k \le 23$	$0 \le k \le 24$	$-23 \le k \le 24$
	$0 \le l \le 24$	$0 \le l \le 28$	$-28 \le l \le 28$
Reflections collected	31428	13309	27586
Independent reflections	4951	12909	9603
	[R(int) = 0.1522]	[R(int)=0.0783]	[R(int) = 0.0283]
Absorption correction	Semi-empirical from equivalents	None	None
Goodness-of-fit on F^2	1.041	1.001	1.063
Final R indices [$I>2\sigma(I)$]	R1 = 0.0654,	R1=0.0428	R1 = 0.0427,
	wR2 = 0.1686	wR2=0.0755	wR2 = 0.1284
R indices (all data)	R1 = 0.1532,	R1=0.0995	R1 = 0.0573,
	wR2 = 0.1978	wR2=0.0798	wR2 = 0.1474

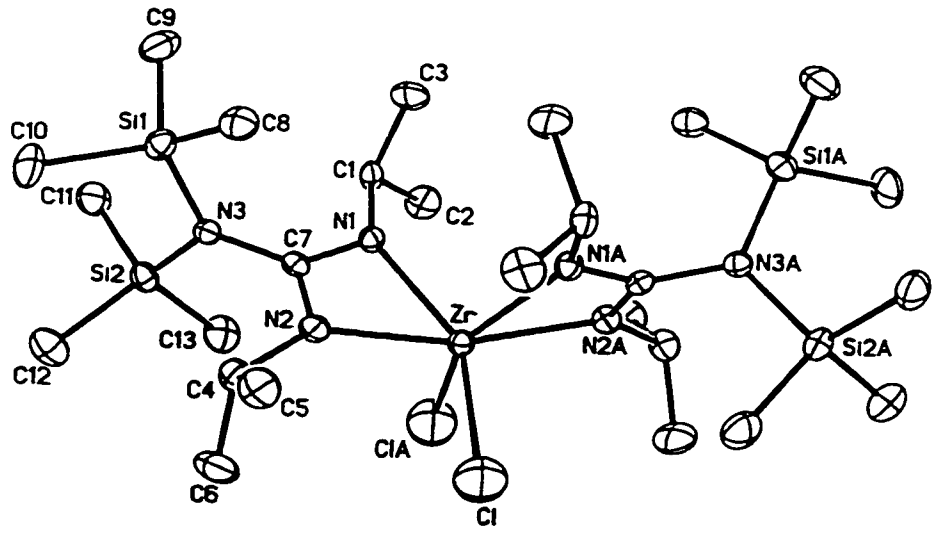

Figure 1. Molecular diagram for $[(^{i}PrN)_2CN(SiMe_3)_2]_2ZrCl_2$ (**1**). Thermal ellipsoids are drawn at 30% probability. Hydrogen atoms have been omitted for clarity.

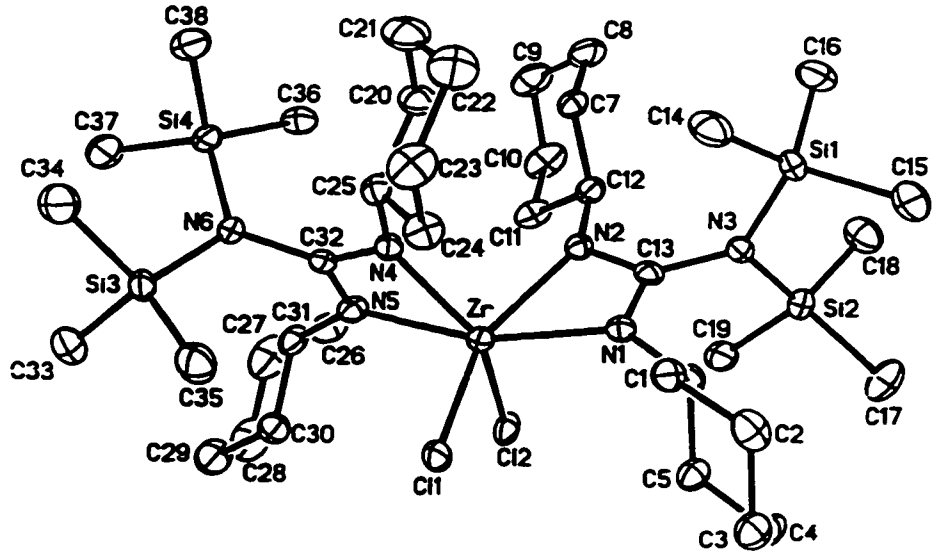

Figure 2. Molecular diagram for $[(CyN)_2CN(SiMe_3)_2]_2ZrCl_2$ (**3**). Thermal ellipsoids are drawn at 30% probability. Hydrogen atoms and solvent of crystallization (toluene) have been omitted for clarity.

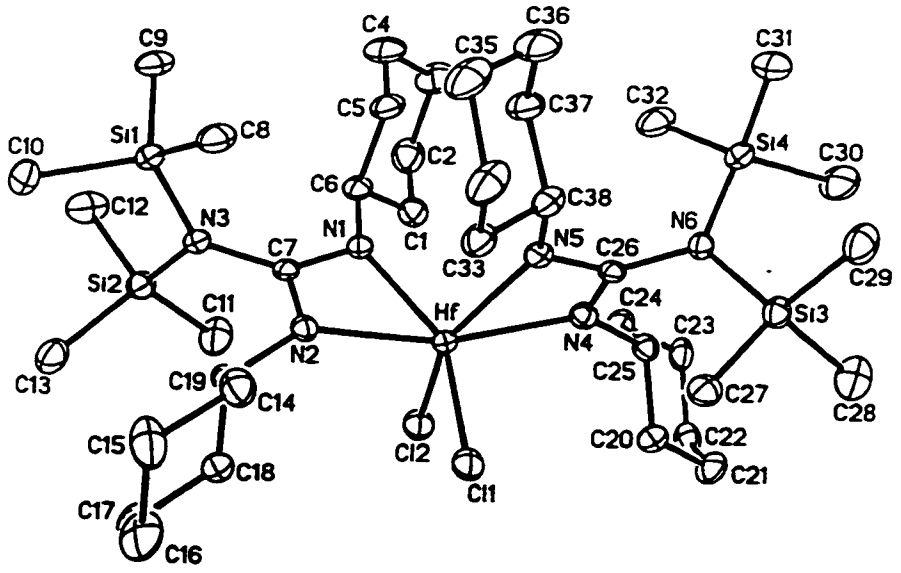

Figure 3. Molecular diagram for $[(CyN)_2CN(SiMe_3)_2]_2HfCl_2$ (**4**). Thermal ellipsoids are drawn at 30% probability. Hydrogen atoms and solvent of crystallization (benzene) have been omitted for clarity.

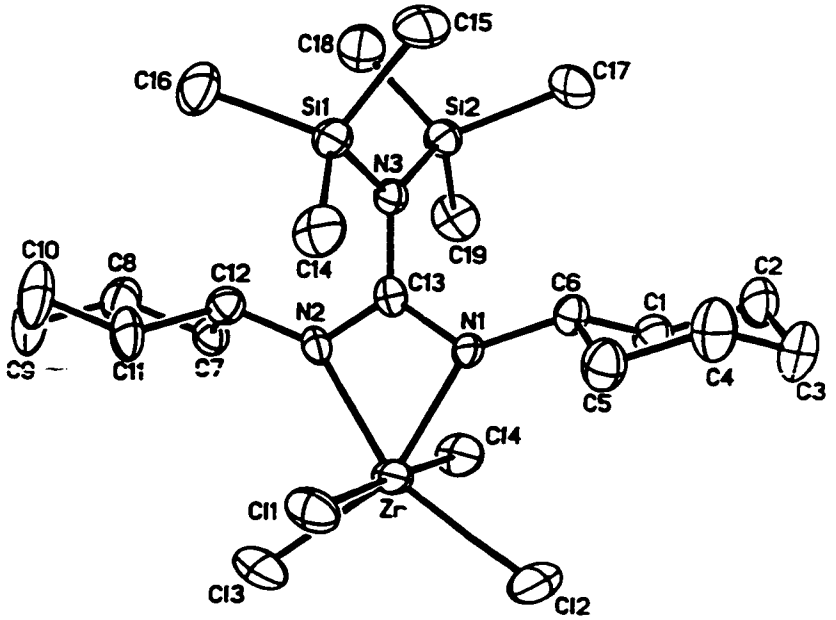

Figure 4. Molecular diagram for $\{[(CyN)_2CN(SiMe_3)_2]ZrCl_4\}^-$ (**5**). Thermal ellipsoids are drawn at 30% probability. Hydrogen atoms and the lithium cation with coordinated solvent molecules have been omitted for clarity.

Table 2. Selected bond lengths [Å] and angles [deg] for $\{^{i}PrNC[N(SiMe_3)_2]N^{i}Pr\}_2ZrCl_2$ (**1**)

Distances			
Zr-N(1)	2.219(4)	N(2)-C(7)	1.343(6)
Zr-N(2)	2.264(4)	N(2)-C(4)	1.480(6)
Zr-Cl	2.420(2)	N(3)-C(7)	1.408(6)
Zr-C(7)	2.700(5)	C(1)-C(2)	1.504(7)
Si(1)-N(3)	1.770(4)	C(1)-C(3)	1.526(8)
Si(2)-N(3)	1.775(4)	C(4)-C(5)	1.494(7)
N(1)-C(7)	1.345(6)	C(4)-C(6)	1.534(8)
N(1)-C(1)	1.462(6)		
Angles			
N(1)A-Zr-N(1)	98.1(2)	ClA-Zr-C(7)	96.13(11)
N(1)A-Zr-N(2)	109.91(14)	C(7)A-Zr-C(7)	131.6(2)
N(1)-Zr-N(2)	59.15(14)	C(7)-N(1)-C(1)	123.0(4)
N(2)A-Zr-N(2)	164.9(2)	C(7)-N(1)-Zr	95.4(3)
N(1)A-Zr-Cl	94.49(12)	C(1)-N(1)-Zr	140.5(3)
N(1)-Zr-Cl	147.82(12)	C(7)-N(2)-C(4)	121.9(4)
N(2)A-Zr-Cl	101.99(12)	C(7)-N(2)-Zr	93.4(3)
N(2)-Zr-Cl	88.73(11)	C(4)-N(2)-Zr	142.7(3)
Cl-Zr-ClA	90.23(12)	C(7)-N(3)-Si(1)	118.8(3)
N(1)A-Zr-C(7)A	29.72(14)	C(7)-N(3)-Si(2)	119.6(3)
N(1)-Zr-C(7)A	109.37(15)	Si(1)-N(3)-Si(2)	121.6(2)
N(2)A-Zr-C(7)A	29.77(13)	N(1)-C(1)-C(2)	109.4(4)
N(2)-Zr-C(7)A	139.49(15)	N(1)-C(1)-C(3)	110.4(4)
Cl-Zr-C(7)A	96.13(11)	C(2)-C(1)-C(3)	110.3(5)
ClA-Zr-C(7)A	118.13(12)	N(2)-C(4)-C(5)	111.1(4)
N(1)A-Zr-C(7)	109.37(14)	N(2)-C(4)-C(6)	110.6(4)
N(1)-Zr-C(7)	29.72(14)	C(5)-C(4)-C(6)	109.8(5)
N(2)A-Zr-C(7)	139.49(15)	N(2)-C(7)-N(1)	110.8(4)
N(2)-Zr-C(7)	29.77(13)	N(2)-C(7)-N(3)	125.2(4)
Cl-Zr-C(7)	118.13(12)	N(1)-C(7)-N(3)	124.0(4)

Table 3. Selected bond lengths [Å] and angles [deg] for $\{CyNC[N(SiMe_3)_2]NCy\}_2ZrCl_2$ (3)

Distances			
Zr-N(4)	2.1991(19)	N(1)-C(6)	1.471(3)
Zr-N(2)	2.213(2)	N(2)-C(13)	1.334(3)
Zr-N(1)	2.216(2)	N(2)-C(12)	1.462(3)
Zr-N(5)	2.232(2)	N(3)-C(13)	1.413(3)
Zr-Cl(1)	2.4229(8)	N(4)-C(32)	1.331(3)
Zr-Cl(2)	2.4259(8)	N(4)-C(25)	1.463(3)
Zr-C(13)	2.670(3)	N(5)-C(32)	1.348(3)
Zr-C(32)	2.672(3)	N(5)-C(31)	1.471(3)
N(1)-C(13)	1.335(3)	N(6)-C(32)	1.418(3)
Angles			
N(4)-Zr-N(2)	94.91(7)	C(13)-N(1)-Zr	94.24(16)
N(4)-Zr-N(1)	108.25(7)	C(6)-N(1)-Zr	141.16(16)
N(2)-Zr-N(1)	59.46(7)	C(13)-N(2)-C(12)	122.5(2)
N(4)-Zr-N(5)	59.67(7)	C(13)-N(2)-Zr	94.37(15)
N(2)-Zr-N(5)	108.04(7)	C(12)-N(2)-Zr	141.79(17)
N(1)-Zr-N(5)	163.40(7)	C(13)-N(3)-Si(2)	118.60(16)
N(4)-Zr-Cl(1)	93.02(6)	C(13)-N(3)-Si(1)	119.33(15)
N(2)-Zr-Cl(1)	149.20(6)	Si(2)-N(3)-Si(1)	121.95(12)
N(1)-Zr-Cl(1)	89.80(5)	C(32)-N(4)-C(25)	122.1(2)
N(5)-Zr-Cl(1)	101.65(5)	C(32)-N(4)-Zr	95.20(15)
N(4)-Zr-Cl(2)	148.32(6)	C(25)-N(4)-Zr	141.71(16)
N(2)-Zr-Cl(2)	94.62(5)	C(32)-N(5)-C(31)	121.5(2)
N(1)-Zr-Cl(2)	102.61(5)	C(32)-N(5)-Zr	93.27(15)
N(5)-Zr-Cl(2)	88.66(5)	C(31)-N(5)-Zr	141.05(16)
Cl(1)-Zr-Cl(2)	94.06(3)	C(32)-N(6)-Si(4)	118.65(16)
N(4)-Zr-C(13)	106.46(7)	C(32)-N(6)-Si(3)	119.72(16)
N(2)-Zr-C(13)	29.89(7)	Si(4)-N(6)-Si(3)	121.63(12)
N(1)-Zr-C(13)	29.90(7)	N(2)-C(13)-N(1))	110.8(2
N(5)-Zr-C(13)	137.75(8)	N(2)-C(13)-N(3)	123.9(2)
Cl(1)-Zr-C(13)	119.60(6)	N(1)-C(13)-N(3)	125.3(2)
Cl(2)-Zr-C(13)	96.65(5)	N(2)-C(13)-Zr	55.74(12)
N(4)-Zr-C(32)	29.75(7)	N(1)-C(13)-Zr	55.86(13)
N(2)-Zr-C(32)	106.22(7)	N(3)-C(13)-Zr	170.32(16)
N(1)-Zr-C(32)	137.77(7)	N(4)-C(32)-N(5)	110.8(2)
N(5)-Zr-C(32)	30.23(7)	N(4)-C(32)-N(6)	124.8(2)
Cl(1)-Zr-C(32)	95.24(5)	N(5)-C(32)-N(6)	124.4(2)
Cl(2)-Zr-C(32)	118.72(6)	N(4)-C(32)-Zr	55.05(12)
C(13)-Zr-C(32)	128.62(7)	N(5)-C(32)-Zr	56.50(12)
C(13)-N(1)-C(6)	121.4(2)	N(6)-C(32)-Zr	170.91(16)

Table 4. Selected bond lengths [Å] and angles [deg] for $\{CyNC[N(SiMe_3)_2]NCy\}_2HfCl_2$ (**4**)

Distances			
Hf-N(1)	2.181(4)	N(1)-C(6)	1.465(7)
Hf-N(5)	2.202(5)	N(2)-C(7)	1.339(7)
Hf-N(4)	2.211(5)	N(2)-C(19)	1.468(7)
Hf-N(2)	2.215(5)	N(3)-C(7)	1.418(7)
Hf-Cl(2)	2.411(2)	N(4)-C(26)	1.344(7)
Hf-Cl(1)	2.414(2)	N(4)-C(25)	1.461(7)
Hf-C(7)	2.656(5)	N(5)-C(26)	1.338(7)
Hf-C(26	2.666(5)	N(5)-C(38)	1.461(7)
N(1)-C(7)	1.342(7)	N(6)-C(26)	1.404(7)
Angles			
N(1)-Hf-N(5)	95.1(2)	N(2)-Hf-C(26)	137.5(2)
N(1)-Hf-N(4)	108.0(2)	Cl(2)-Hf-C(26)	120.42(12)
N(5)-Hf-N(4)	59.9(2)	Cl(1)-Hf-C(26)	95.80(12)
N(1)-Hf-N(2)	60.1(2)	C(7)-Hf-C(26)	128.8(2)
N(5)-Hf-N(2)	107.7(2)	C(7)-N(1)-C(6)	121.5(5)
N(4)-Hf-N(2)	163.5(2)	C(7)-N(1)-Hf	94.9(3)
N(1)-Hf-Cl(2)	92.54(13)	C(6)-N(1)-Hf	142.7(4)
N(5)-Hf-Cl(2)	150.16(13)	C(7)-N(2)-C(19)	121.8(5)
N(4)-Hf-Cl(2)	90.35(13)	C(7)-N(2)-Hf	93.4(3)
N(2)-Hf-Cl(2)	101.12(13)	C(19)-N(2)-Hf	140.5(4)
N(1)-Hf-Cl(1)	149.51(13)	C(7)-N(3)-Si(2)	120.1(4)
N(5)-Hf-Cl(1)	94.09(13)	C(7)-N(3)-Si(1)	118.8(4)
N(4)-Hf-Cl(1)	101.78(14)	Si(2)-N(3)-Si(1)	121.2(3)
N(2)-Hf-Cl(1)	89.38(12)	C(26)-N(4)-C(25)	121.3(5)
Cl(2)-Hf-Cl(1)	93.81(7)	C(26)-N(4)-Hf	94.0(3)
N(1)-Hf-C(7)	30.2(2)	C(25)-N(4)-Hf	141.2(4)
N(5)-Hf-C(7)	106.2(2)	C(26)-N(5)-C(38)	122.1(5)
N(4)-Hf-C(7)	138.0(2)	C(26)-N(5)-Hf	94.6(3)
N(2)-Hf-C(7)	30.2(2)	C(38)-N(5)-Hf	142.1(4)
Cl(2)-Hf-C(7)	94.69(12)	C(26)-N(6)-Si(3)	118.4(4)
Cl(1)-Hf-C(7)	119.41(12)	C(26)-N(6)-Si(4)	119.9(4)
N(1)-Hf-C(26)	106.5(2)	Si(3)-N(6)-Si(4)	121.6(3)
N(5)-Hf-C(26)	30.0(2)	N(2)-C(7)-N(1)	110.5(5)
N(4)-Hf-C(26)	30.2(2)	N(2)-C(7)-N(3)	124.7(5)
		N(1)-C(7)-N(3)	124.8(5)

Charge compensation for these anionic complexes is provided in both cases by a Li cation, which is associated with one of the chloro ligands (Li-Cl(1) 2.39(2)° in **5** and Li-Cl(4) 2.42(6)° in **6**). Tetrahydrofuran or a combination of diethyl ether and THF complete the coordination spheres of the Li cations.

The reaction of **5** with three equivalents of $PhCH_2MgCl$ proceeded according to the metathesis reaction shown in Scheme 2 to yield complex **7**. Spectroscopic characterization indicated the incorporation of three benzyl groups and was consistent with the formulation of this species as $\{CyNC[N(SiMe_3)_2]NCy\}Zr(CH_2Ph)_3$. Both the ^{13}C and ^{1}H NMR spectra indicated a single Cy substituent and a single benzyl group and gave no evidence of an η^2-benzyl ligand.

The molecular structure of **7** was determined and an ORTEP diagram is provided in Figure 6 and crystallographic data is summarized in Tables 5 and 8. The geometry of the five coordinate Zr center is better described as a distorted tetrahedral with vertices defined by the three benzyl groups and the central carbon (C13) of the guanidinate ligand. The corresponding angles range from 118.2(3)° to 90.7(2)° with an average value of 107.8°.

The average $Zr\text{-}CH_2$ bond distance is 2.273(6) Å which is shorter than the corresponding distances in the recently reported β-ketimino complex $(TTP)Zr(CH_2Ph)_3$ (TTP = 2-p-tolylamino-4-p-tolylimino-2-pentenato) which averaged 2.290(5)Å ($Zr\text{-}C\text{-}C_{ipso}$ = 99.1(2)°)[3] or $CpZr(CH_2Ph)_3$ at 2.299(8)Å ($Zr\text{-}C_{ispo}$ 2.818(8)Å $Zr\text{-}C\text{-}C_{ipso}$ = 94.5(5)°).[4]

One of the benzyl groups in **7** is unique in exhibiting a significantly more acute $Zr\text{-}C\text{-}C_{ipso}$ angle (Zr-C(20)-C(26) 88.7(4)° vs. Zr-C(27)-C(33) 116.0(5)° and Zr-C(34)-C(40)

Table 5. Crystallographic Data for, $\{CyNC[N(SiMe_3)_2]NCy\}ZrCl_4]Li(THF)_2(Et_2O)$ (**5**), $\{CyNC[N(SiMe_3)_2]NCy\}HfCl_4]Li(THF)_3$ (**6**), and $\{CyNC[N(SiMe_3)_2]NCy\}Zr(CH_2Ph)_3$ (**7**)

Empirical formula	$C_{31}H_{66}Cl_4LiN_3O_3Si_2Zr$ (**5**)	$C_{31}H_{64}Cl_4HfLiN_3O_3Si_2$ (**6**)	$C_{40}H_{61}N_3Si_2Zr$ (**7**)
Formula weight	825.01	910.26	731.32
Temperature (K)	203(2)	223(2)	203(2)
Wavelength Å	0.71073	0.71073	0.71073
Crystal system	Orthorhombic	Orthorhombic	Monoclinic
Space Group	Pbcn	Pbcn	$P2_1/n$
Unit cell dimensions (Å, deg)	a = 33.284(7) b = 14.956(3) c = 17.381(4) α = 90 β = 90 γ = 90	a = 33.460(2) b = 15.0033(8) c = 17.3857(9) α = 90 β = 90 γ = 90	a = 10.483(1) b = 18.889(2) c = 20.459(3) α = 90 β = 102.431(2) γ = 90
Volume ($Å^3$)	8652(3)	8727.8(8)	3956.0(9)
Z	8	8	4
Density (Mg/m^3) (calculated)	1.267	1.385	1.228
Absorption coefficient (mm^{-1})	0.588	2.721	0.369
F(000)	3488	3728	1560
Crystal size (mm)	0.2 x 0.2 x 0.3	0.20 x 0.20 x 0.20	0.1 x 0.1 x 0.06
Limiting indices	0≤h≤33 0≤k≤15 0≤l≤17	-38≤h≤43 -10≤k≤20 -22≤l≤23	-10≤h≤10 0≤k≤18 0≤l≤20
Reflections collected	4642	20951	30927
Independent reflections	4642 [R(int) = 0.0932]	4077 [R(int) = 0.0551]	4145 [R(int) = 0.2136]
Absorption correction	Semi-empirical from equivalents	None	Semi-empirical from equivalents
Goodness-of-fit on F^2	1.016	1.183	1.027
Final R indices [I>2σ(I)]	R1 = 0.0802, wR2 = 0.2408	R1 = 0.0937, wR2 = 0.2385	R1 = 0.0473 wR2 = 0.0918
R indices (all data)	R1 = 0.0946, wR2 = 0.2532	R1 = 0.1039, wR2 = 0.2458	R1 = 0.0878 wR2 = 0.1003

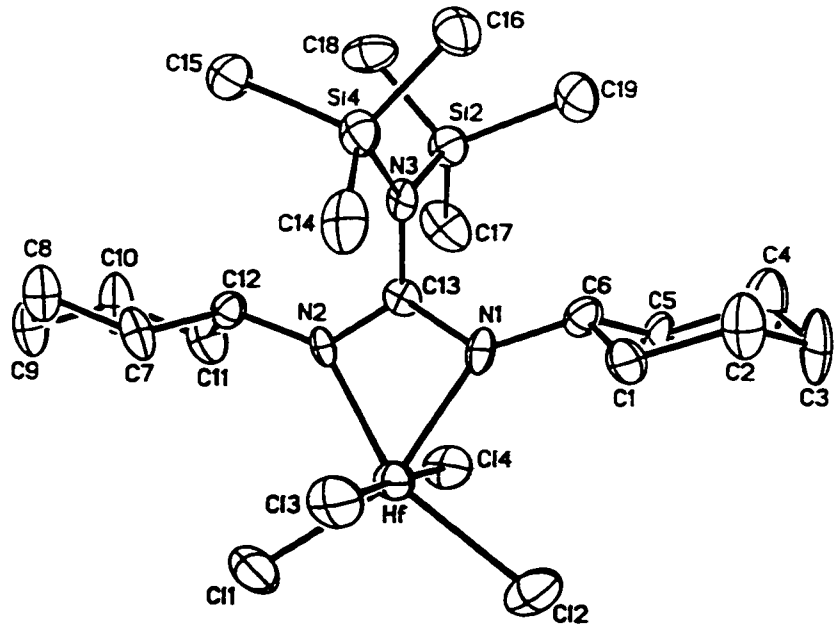

Figure 5. Molecular diagram for $\{[(CyN)_2CN(SiMe_3)_2]HfCl_4\}^-$ (**6**). Thermal ellipsoids are drawn at 30% probability. Hydrogen atoms and the lithium cation with coordinated solvent molecules have been omitted for clarity.

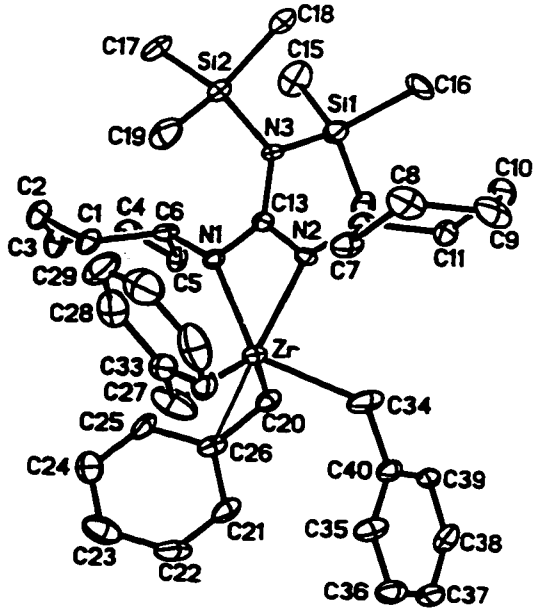

Figure 6. Molecular diagram for $[(CyN)_2CN(SiMe_3)_2]ZrBz_3$ (**7**). Thermal ellipsoids are drawn at 30% probability. Hydrogen atoms have been omitted for clarity.

Table 6. Bond lengths [A] and angles [deg] for [{CyNC[N(SiMe$_3$)$_2$]NCy}ZrCl$_4$][Li(THF)$_2$(Et$_2$O)] (**5**)

Distances			
Zr-N(2)	2.179(7)	Si(2)-C(19)	1.852(9)
Zr-N(1)	2.181(6)	Si(2)-C(18)	1.849(10)
Zr-Cl(4)	2.423(2)	Si(2)-C(17)	1.862(9)
Zr-Cl(2)	2.434(3)	Cl(1)-Li	2.39(2)
Zr-Cl(3)	2.441(3)	Li-O(1)	1.97(3)
Zr-Cl(1)	2.544(2)	Li-O(3)	1.92(3)
Zr-C(13)	2.641(9)	Li-O(2)	1.95(2)
Si(1)-N(3)	1.758(6)	N(1)-C(13)	1.312(10)
Si(1)-C(14)	1.855(9)	N(1)-C(6)	1.466(10)
Si(1)-C(16)	1.849(9)	N(2)-C(13)	1.336(10)
Si(1)-C(15)	1.889(9)	N(2)-C(12)	1.469(10)
Si(2)-N(3)	1.768(6)	N(3)-C(13)	1.426(11)
Angles			
Si(1)-N(3)-Si(2)	124.0(4)	Cl(2)-Zr-C(13)	124.80(19)
N(1)-C(13)-N(2)	110.7(7)	Cl(3)-Zr-C(13)	127.72(19)
N(1)-C(13)-N(3)	125.3(7)	Cl(1)-Zr-C(13)	89.07(15)
N(2)-C(13)-N(3)	124.0(7)	N(3)-Si(1)-C(14)	108.4(4)
N(1)-C(13)-Zr	55.4(4)	N(3)-Si(1)-C(16)	113.5(4)
N(2)-C(13)-Zr	55.4(4)	C(13)-N(1)-C(6)	123.6(7)
N(3)-C(13)-Zr	177.7(5)	C(13)-N(1)-Zr	94.9(5)
N(2)-Zr-N(1)	60.0(2)	C(6)-N(1)-Zr	141.4(5)
N(2)-Zr-Cl(4)	92.77(18)	C(13)-N(2)-C(12)	123.7(7)
N(1)-Zr-Cl(4)	93.07(17)	C(13)-N(2)-Zr	94.3(5)
N(2)-Zr-Cl(2)	155.00(19)	C(12)-N(2)-Zr	141.9(5)
N(1)-Zr-Cl(2)	95.14(18)	C(13)-N(3)-Si(1)	118.0(5)
Cl(4)-Zr-Cl(2)	90.70(10)	C(13)-N(3)-Si(2)	117.9(5)
N(2)-Zr-Cl(3)	97.49(18)	C(13)-N(1)-C(6)	123.6(7)
N(1)-Zr-Cl(3)	157.15(18)	C(13)-N(1)-Zr	94.9(5)
Cl(4)-Zr-Cl(3)	91.63(9)	C(6)-N(1)-Zr	141.4(5)
Cl(2)-Zr-Cl(3)	107.16(11)	C(13)-N(2)-C(12)	123.7(7)
N(2)-Zr-Cl(1)	89.18(18)	C(13)-N(2)-Zr	94.3(5)
N(1)-Zr-Cl(1)	88.60(17)	C(12)-N(2)-Zr	141.9(5)
Cl(4)-Zr-Cl(1)	177.89(9)	C(13)-N(3)-Si(1)	118.0(5)
Cl(2)-Zr-Cl(1)	87.87(10)	C(13)-N(3)-Si(2)	117.9(5)
Cl(3)-Zr-Cl(1)	87.32(9)	C(13)-N(1)-C(6)	123.6(7)
N(2)-Zr-C(13)	30.3(2)	C(13)-N(1)-Zr	94.9(5)
N(1)-Zr-C(13)	29.7(2)	C(6)-N(1)-Zr	141.4(5)
Cl(4)-Zr-C(13)	93.01(15)	C(13)-N(2)-C(12)	123.7(7)
		C(13)-N(2)-Zr	94.3(5)

Table 7. Selected bond lengths [Å] and angles [deg] for [{CyNC[N(SiMe$_3$)$_2$]NCy}HfCl$_4$][Li(THF)$_3$] (**6**)

Distances			
Hf-N(2)	2.17(2)	N(1)-C(13)	1.32(2)
Hf-N(1)	2.19(2)	N(1)-C(6)	1.42(2)
Hf-Cl(3)	2.402(6)	N(2)-C(13)	1.34(2)
Hf-Cl(1)	2.427(6)	N(2)-C(12)	1.46(2)
Hf-Cl(2)	2.424(6)	N(3)-C(13)	1.41(2)
Hf-Cl(4)	2.524(5)	N(3)-Si(2)	1.759(14)
Hf-C(13)	2.63(2)	N(3)-Si(4)	1.79(2)
		Li-Cl(4)	2.42(6)
Angles			
Cl(4)-Hf-C(13)	89.2(4)	N(1)-Hf-Cl(2)	97.8(5)
C(13)-N(1)-C(6)	124(2)	Cl(3)-Hf-Cl(2)	91.3(2)
C(13)-N(1)-Hf	94.0(12)	Cl(1)-Hf-Cl(2)	105.8(2)
C(6)-N(1)-Hf	141.5(14)	N(2)-Hf-Cl(4)	88.7(4)
C(13)-N(2)-C(12)	125(2)	N(1)-Hf-Cl(4)	89.4(4)
C(13)-N(2)-Hf	94.3(12)	Cl(3)-Hf-Cl(4)	177.9(2)
C(12)-N(2)-Hf	140.7(13)	Cl(1)-Hf-Cl(4)	87.7(2)
C(13)-N(3)-Si(2)	119.1(12)	Cl(2)-Hf-Cl(4)	87.3(2)
C(13)-N(3)-Si(4)	118.5(11)	N(2)-Hf-C(13)	30.6(6)
Si(2)-N(3)-Si(4)	122.3(10)	N(1)-Hf-C(13)	30.0(5)
N(1)-C(13)-N(2)	111(2)	Cl(3)-Hf-C(13)	92.9(4)
N(2)-Hf-N(1)	60.6(6)	Cl(1)-Hf-C(13)	126.1(5)
N(2)-Hf-Cl(3)	93.2(4)	Cl(2)-Hf-C(13)	127.7(5)
N(1)-Hf-Cl(3)	92.3(4)	N(1)-C(13)-N(3)	126(2)
N(2)-Hf-Cl(1)	95.6(4)	N(2)-C(13)-N(3)	123(2)
N(1)-Hf-Cl(1)	156.1(5)	N(1)-C(13)-Hf	56.0(10)
Cl(3)-Hf-Cl(1)	91.2(2)	N(2)-C(13)-Hf	55.1(10)
N(2)-Hf-Cl(2)	158.0(4)	N(3)-C(13)-Hf	177.0(13)

Table 8. Selected bond lengths [Å] and angles [deg] for {CyNC[N(SiMe$_3$)$_2$]NCy}Zr(CH$_2$Ph)$_3$ (7)

Distances			
Zr-N(1)	2.241(4)	N(1)-C(6)	1.465(6)
Zr-N(2)	2.250(5)	N(2)-C(13)	1.344(7)
Zr-C(27)	2.263(7)	N(2)-C(12)	1.461(6)
Zr-C(20)	2.268(5)	N(3)-C(13)	1.421(7)
Zr-C(34)	2.288(6)	C(20)-C(26)	1.466(8)
Zr-C(26)	2.672(6)	C(21)-C(26)	1.417(8)
Zr-C(13)	2.683(6)	C(25)-C(26)	1.385(8)
Si(1)-N(3)	1.756(5)	C(27)-C(33)	1.463(9)
Si(2)-N(3)	1.775(4)	C(34)-C(40)	1.491(8)
N(1)-C(13)	1.339(7)		
Angles			
N(1)-Zr-N(2)	59.77(17)	C(13)-N(1)-C(6)	122.7(5)
N(1)-Zr-C(27)	111.7(3)	C(13)-N(1)-Zr	93.7(3)
N(2)-Zr-C(27)	113.8(2)	C(6)-N(1)-Zr	143.3(4)
N(1)-Zr-C(20)	95.6(2)	C(13)-N(2)-C(12)	122.2(5)
N(2)-Zr-C(20)	126.4(2)	C(13)-N(2)-Zr	93.1(4)
C(27)-Zr-C(20)	119.6(3)	C(12)-N(2)-Zr	144.5(4)
N(1)-Zr-C(34)	138.9(2)	C(13)-N(3)-Si(1)	117.1(3)
N(2)-Zr-C(34)	84.0(2)	C(13)-N(3)-Si(2)	119.2(4)
C(27)-Zr-C(34)	99.9(3)	Si(1)-N(3)-Si(2)	123.7(3)
C(20)-Zr-C(34)	90.7(2)	C(2)-C(1)-C(6)	111.4(5)
N(1)-Zr-C(26)	107.20(19)	C(1)-C(2)-C(3)	111.7(5)
N(2)-Zr-C(26)	158.43(18)	N(1)-C(13)-N(2)	113.1(5)
C(27)-Zr-C(26)	86.5(2)	N(1)-C(13)-N(3)	123.6(5)
C(20)-Zr-C(26)	33.3(2)	N(2)-C(13)-N(3)	123.3(6)
C(34)-Zr-C(26)	100.2(2)	N(1)-C(13)-Zr	56.4(3)
N(1)-Zr-C(13)	29.86(16)	N(2)-C(13)-Zr	56.9(3)
N(2)-Zr-C(13)	30.00(16)	N(3)-C(13)-Zr	174.7(4)
C(27)-Zr-C(13)	118.2(2)	C(26)-C(20)-Zr	88.7(4)
C(20)-Zr-C(13)	112.0(2)	C(25)-C(26)-C(21)	116.7(7)
C(34)-Zr-C(13)	111.4(2)	C(25)-C(26)-C(20)	121.2(6)
C(26)-Zr-C(13)	134.14(19)	C(21)-C(26)-C(20)	121.3(6)
N(3)-Si(1)-C(14)	108.7(3)	C(25)-C(26)-Zr	94.2(4)
N(3)-Si(1)-C(15)	110.0(3)	C(21)-C(26)-Zr	110.4(4)
N(3)-Si(1)-C(16)	113.0(3)	C(20)-C(26)-Zr	58.1(3)
N(3)-Si(2)-C(19)	109.0(3)	C(33)-C(27)-Zr	116.0(5)
N(3)-Si(2)-C(18)	108.9(3)	C(40)-C(34)-Zr	123.2(4)
N(3)-Si(2)-C(17)	112.3(3)		

123.2(4)°) and a short Zr-C_{ipso} [Zr-C(26)] distance of 2.672(6)Å. These features establish that the phenyl group of this moiety is a weak electron donor and contrast with those in (TTP)Zr(CH_2Ph)$_3$ (Zr-C-C_{ipso} = 99.1(2)°)[3] and $CpZr(CH_2Ph)_3$ at 2.299(8)Å (Zr-C_{ispo} 2.818(8)Å Zr-C-C_{ipso} = 94.5(5)°)[4] possibly indicating that the Zr center in **7** is more electron deficient than in these complexes. Supporting this is the observation of similar bonding parameters observed in related tribenzyl complexes supported by bulky aryloxides in which the η^2-benzyl exhibited a Zr-C-C_{ipso} angle of 84.3(9)° (Zr-CH_2 2.28Å, Zr-C_{ispo} 2.59Å)[5] and the structurally characterized cationic species $[Cp_2Zr(CH_2Ph)NCCH_3]^+$ (Zr-CH_2 2.344(8)Å, Zr-C_{ispo} 2.648(6)Å, Zr-C-C_{ipso} = 84.9(4)°)[6] For reference, $Zr(CH_2Ph)_4$ exhibits a mean Zr-C-C_{ipso} of 92(1)° (range from 85-101°).[7]

The possibility of a significant π interaction between the planar $N(SiMe_3)_2$ function of the guanidinate and the bidentate NCN fragment can be ruled out on the basis of the observed dihedral angle of 85.8(3)°.

In summary, guanidinate ligands have proven to be useful in the preparation of a family of bis(guanidinate) and anionic mono(guanidinate) group 4 complexes. A combination of x-ray crystallographic and spectroscopic studies confirm the C_2 symmetric features of the bis(guanidinate) compounds and the structures of the mono(guanidinate) species. From these results, it is clear that little conjugation occurs between the lone pair on the planar NR'_2 group and the guanidinate NCN π system. The nearly perpendicular orientation of the NR'_2 substituents to the MNCN plane results in a system that appears to exhibit steric features within the plane of the ligand that are similar to $[RNC(Me)NR]^-$.

References

(1) Littke, A.; Sleiman, N.; Bensimon, C.; Richeson, D. S.; Yap, G. P. A.; Brown, S. *Organometallics* **1998**, 17, 446

(2) Prout, K.; Cameron, T. S.; Forder, R. A.; Critchley, S. R.; Denton, B.; Rees, G. V. *Acta Cryst.* **1974**, B30, 2290

(3) Qian, B.; Scanlon, IV, W. J.; Smith, III, M. R.; Motry, D. H. *Organometallics* **1999**, 18, 1693

(4) Scholz, J.; Rehbaum, F.; Theile, K.-H.; Goddard, R.; Betz, P.; Krüger, C. *J. Organomet. Chem.* **1993**, 443, 93

(5) Latesky, S. L.; McMullen, A. K.; Niccolai, G. P.; Rothwell, I. P.; Huffman, J. C. *Organometallics*, **1985**, 4, 902

(6) (a) Jordan, R. F.; Lapointe, R. E.; Baenziger, N.; Hinch, G. D.. *Organometallics.* **1990**, 9, 1539

(b) Jordan, R. F.; Lapointe, R. E.; Bajgur, C. S.; Echols, S. F.; Willett, R. *J. Am. Chem. Soc.* **1987**, 109, 4111

(7) Davies, G. R.; Jarvis, J. A. J.; Kilbourn, B. T. *J. Chem. Soc., Chem. Commun.* **1971**, 1511

Chapter 3

Protonation Pathways to Group 5 Transition Metal Guanidinate Complexes

Introduction

In this chapter we move to a trialkyl substituted guanidine, specifically triisopropyl guanidine. In contrast to the tetra-substituted analogues, these species have potential to yield dianionic species by deprotonation of a second N-H function. In addition, relative to the trimethylsilyl groups, the alkyl groups, through inductive effects, may increase the donor ability of the ligand (Scheme 1). This dianionic ligand could function as a diamido ligand and is isoelectronic with the carbonate anion and the trimethylenemethane dianion and may exhibit similar π delocalization (Y-conjugation) of the lone pairs on the sp^2 hybridized nitrogen centers, (**I**, Scheme 1). In addition to possessing interesting electronic features, we felt that these species would be simple to handle, impart solubility of metal complexes in organic solvents and that substituent modification may allow investigation of deliberate variations to the steric parameters of the ligand and its metal complexes.

Among the routes available for the introduction of trialkylguanidinate anions and dianions into a metal coordination sphere, direct reaction of the two active N-H protons of a N, N', N''–trialkylguanidine in a protonation/elimination reaction with precursor metal complexes is particularly attractive. Metal alkyl moieties should be susceptible to such protonation/elimination reactions and are synthetically appealing from the standpoint of generating volatile, and thus easily removable, side products. Although only one example of alkyl elimination can be found in the literature,[1] an alkyl group should be basic enough to deprotonate the guanidine ligands N-H function and should follow a pathway similar to the recently published elimination reaction involving dimethylamido groups (Equation 1).[2]

In this chapter the *in situ* reaction of Nb and Ta alkyl complexes, Me_xMCl_y (M = Ta, x = 3, y = 2; M = Nb, x = 2, y = 3), with N, N', N''–triisopropylguanidine are reported.

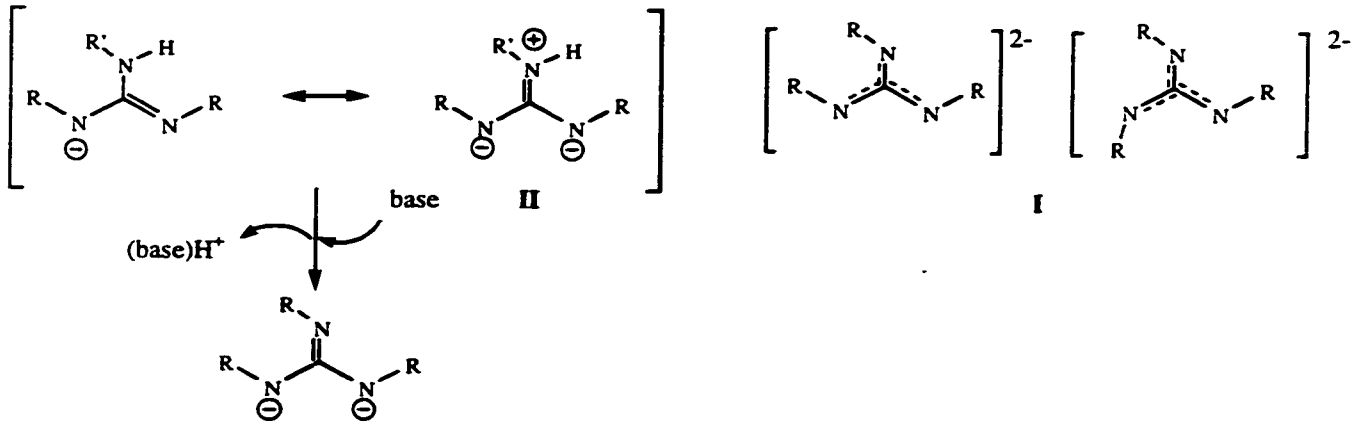

Scheme 1

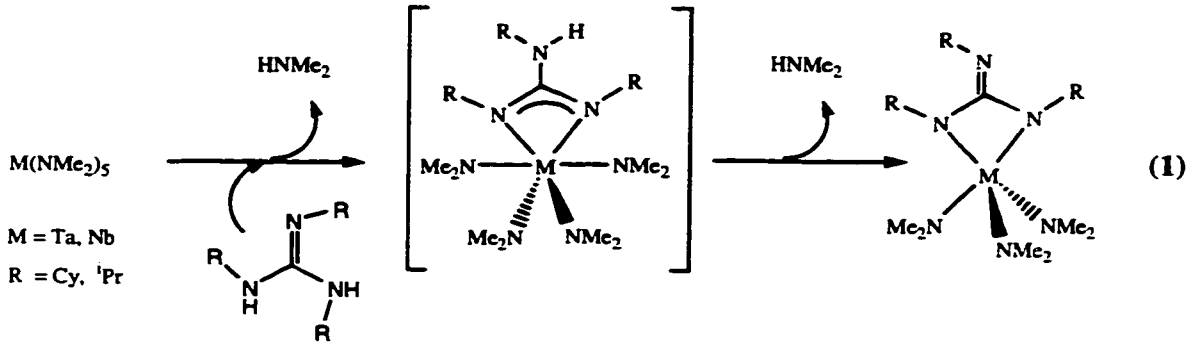

(1)

Experimental

General Considerations

All manipulations were carried out in either a nitrogen filled drybox or under nitrogen using standard Schlenk-line techniques. Solvents were distilled under nitrogen from Na/K alloy. Preparation of Me_3TaCl_2 and Me_2NbCl_3 was carried out according to literature procedures.[3] ^1H NMR spectra were run on either a Gemini 200 MHz with deuterated benzene

or pyridine as a solvent and internal standard. All elemental analyses were run on a Perkin Elmer PE CHN 4000 elemental analysis system.

$NbMe_2Cl_2[(^iPrN)_2C(NH^iPr)]$ (1)

$ZnMe_2$ (4.1ml, 2 M in toluene) was added to a mixture of $NbCl_5$ (2.000 g, 7.40 mmol) in 40-ml pentane and allowed to stir for 24 hours. Filtration gave an orange solution of Me_2NbCl_3. To this solution was added triisopropylguanidine (1.372 g, 7.40 mmol) which had been dissolved in 15-ml pentane. The resulting mixture was allowed to stir for another 24 hours. Filtration gave an orange solid (2.41 g). To the orange solid CH_2Cl_2 was added, leaving behind a gray insoluble compound and giving a soluble red liquid. Concentration of solution gave blood red crystals of **1** (1.12 g, 40.0%).

^1H NMR (py-d_5): 4.48 (sept, CH, 2H), 3.95 (br, CH, 1H), 2.36 (s, Nb-CH_3), 1.52 (d, CH_3, 12H), 1.27 (d, CH_3, 6H)

^{13}C NMR (py-d_5): 171.5 (s, N_3C), 79.1 (br, Nb-CH_3), 48.4, 45.6 (2s, CH), 23.7, 22.9 (2s, CH_3)

$NbMeCl_3[(^iPrN)_2C(NH^iPr)]$ (2)

Trace amounts were isolated in the filtrate from the preparation of **1**. Orange crystals suitable for x-ray were obtained from toluene. However there was an insufficient amount for spectroscopic studies and microanalysis.

$NbMe_3Cl[(^iPrN)_2C(NH^iPr)]$ (3)

Compound **1** (0.182 g, 0.48 mmol) was placed into 10-ml hexane and cooled to -35°C. MeLi (0.34 ml, 1.4M in diethylether) was added and the reaction was allowed to stir

and warm to room temperature over 45 minutes. Filtration yielded a dark brown solid of **3**. Orange crystals could be obtained, suitable for XRD, from toluene. However a spectroscopically pure sample have yet to be obtained.

$TaMe_3Cl[(^iPrN)_2C(NH^iPr)]$ (4)

$TaCl_5$ (0.01 mol, 3.582 g) was placed into 30-ml pentane and $ZnMe_2$ (1.6 mmol, 7.9 ml, 2 M in toluene) was added via a syringe. After one hour the mixture was filtered to give a very pale yellow solution which should contain Me_3TaCl_2. Triisopropylguanidine (0.01 mol, 1.853 g) dissolved in pentane was added to this solution via a pipette. Immediate filtration yielded a light yellow solid (2.525 g, 5.7 mmol). Addition of 20 ml of toluene and filtration of insoluble material followed by concentration of the filtrate and cooling to -35°C gave (2.21 g, 49.6% yield) of light yellow crystals of **4**.

^1H NMR (C_6D_6) 4.17 (sept, CH, 2 H), 3.85 (br, NH, 1 H), 3.45 (mult, CH, 1 H), 1.58 (s, Ta-CH_3, 9 H), 1.25 (d, CH_3, 12 H), 0.80 (d, CH_3, 6 H)

^{13}C NMR (C_6D_6) 169.63 (s, N_3C), 81.86 (s, Ta-CH_3), 48.94, 47.59 (2s, CH), 23.62, 23.01 (2s, CH_3)

EA: Calculated for $TaN_3ClC_{13}H_{31}$: C 35.02; H 7.01; N 9.43. Found: C 34.42; H 6.96; N 9.32

$TaMe_4[(^iPrN)_2C(NH^iPr)]$ (5)

To a solution of **4** (0.197 g, 0.44 mmol) dissolved in 10 ml of toluene and cooled to -35°C, MeLi (0.34 ml, 1.4 M in diethyl ether) was added. The mixture was allowed to warm to room temperature after 1.5 hours and then sit at room temperature for 1.5 hours. Filtration and removal of the pale yellow solution gave a yellow solid. Yellow crystals of **5** were obtained from pentane (0.101 g, 54% yield) at -35°C.

^{1}H NMR (C_6D_6) 3.87 (sept, CH, 2 H), 3.33 (br, CH and NH, 3 H), 1.38 (s, CH_3, 12 H), 1.14 (d, CH_3, 12 H), 0.74 (d, CH_3, 6 H)

^{13}C NMR (C_6D_6) 167.23 (s, N_3C), 78.93 (s, Ta-CH_3), 47.80, 46.78 (2s, CH), 23.73, 23.55 (2s, CH_3)

EA: Calculated for $TaN_3C_{14}H_{34}$: C 39.53; H 8.06; N 9.88. Found: C 38.66; H 7.68; N 10.69

Results and Discussion

Among the issues raised in employing $M(NMe_2)_5$ and $Ta(NMe_2)_4Cl$ in reactions with guanidines was the fact that the third nitrogen atom of the resultant dianionic guanidinate ligand did not become involved in bonding with the metal.[2] The presence of the strongly π donating amido ligands which have reduced the electron deficiency of the metal center may offer an explanation for these observations. In addition, the steric congestion provided by the amido ligands may be a further reason for the lack of coordination of the third nitrogen atom. To address the role of π donors in guanidinate complexes we attempted to prepare analogue complexes in which the amido ligands have been replaced by the none π donating methyl ligands. Furthermore, we hoped to gain insight into the factors that influence monoanionic *vs.* dianionic guanidinate formation.

These efforts began with the selection of Ta and Nb alkyl complexes and, based on several factors such as ease of synthesis and purification, the reported compounds Me_2NbCl_3 and Me_3TaCl_2 were chosen as starting materials.[3] The preparation of these materials relies on the reaction of slightly greater than stoichiometric amounts of $ZnMe_2$ with MCl_5. The products of these reactions are a result of an equilibrium process, and their ratios are highly

dependent on solubility and time. The equilibrium process involved in the preparation of Me_2NbCl_3 is shown as an example (Equation 2).

Overall:

$$NbCl_5 + 1.1\ ZnMe_2 \xrightarrow[24h]{\text{pentane}} NbMe_2Cl_3 + 1.1\ ZnCl_2 \qquad (2)$$

Mechanism:

$$NbCl_5 + ZnMe_2 \longrightarrow NbMe_3Cl_2 + ZnCl_2$$

$$NbCl_5 + 2\ Me_3NbCl_2 \longrightarrow 3\ Me_2NbCl_2$$

The reaction of Me_2NbCl_3 or Me_3TaCl_2 with one equivalent of N, N', N"-triisopropylguanidine proceeded rapidly at room temperature to yield the products shown in Scheme 2 and 3.

Both ^1H and ^{13}C NMR spectra for these new compounds (**1-5**) confirmed the incorporation of guanidine ligands into the products and gave ^iPr resonances in a 2:1 ratio. Such a pattern has been observed for a fluxional monoanionic guanidinate ligand. This was a surprising contrast to the results previously obtained in similar reactions with $M(NMe_2)_5$ (M = Nb, Ta) in which two dimethylamido ligands were rapidly protonated and eliminated from the starting metal complex. However it was similar to observations made in the case of reactions with $Ta(NMe_2)_4Cl$.[4] Furthermore, these spectra indicated that some metal-methyl functions remained in all of the products.

The synthetic procedure for the preparation of compounds **1** and **4** employs *in situ* generated Nb and Ta alkyl species (i.e. Me_2NbCl_3 and Me_3TaCl_2) in reactions with

guanidines. This methodology consistently yielded a major product with one additional methyl function bonded to the metal than was anticipated from the reported starting materials. For example, employing the reported procedure for synthesis of Me_2NbCl_3 followed by direct addition of guanidine to the reaction solution resulted in isolation of **1** according to Scheme 2. Similarly, using an *in situ* source of Me_3TaCl_2 resulted in isolation of **4** as the major product. Both **1** and **4** contain one additional methyl substituent bonded to the metal center as was indicated clearly in the NMR spectra of **1** and **4**. The integrated intensity and peak positions also clearly indicate one methyl peak showing a fluxional species integrating for 6 and 9 hydrogens respectively. The 2:1 isopropyl signals and the presence of an N-H signal help confirm that the compounds contain a monoanionic guanidine. Interestingly, only a trace of the expected species **2** was observed from these attempts.

Several complexes could be isolated as single crystals. In some cases only trace amounts were obtained. X-ray crystallographic analyses of **1**, **2**, **3**, and **4** confirmed the identities and structural features of these products with the results of these studies provided in Figures 1-4 and Tables 1-5.

Complex **1** was the major product isolated by the procedure employed in these reactions. X-ray data for **1** indicated that it was a pseudo-octahedral species having equatorial groups N(1), N(2), C(12), and Cl(2) and axial chloride Cl(1) and methyl C(11) ligands. The guanidinate ligand exhibited a bite angle of 62.49(12)°. The structural parameters around the uncoordinated N(3) atom (C(7)-N(3)-C(10) = 129.7(3)° and N(3)-C(10) = 1.326(5)Å) as well as the dihedral angle between the C(10)-N(3)-C(7) plane and the N(1)-C(10)-N(2) plane of 18.3° are consistent with N(3) being sp^2 hybridized and some degree of π-overlap with N(3) and C(10).

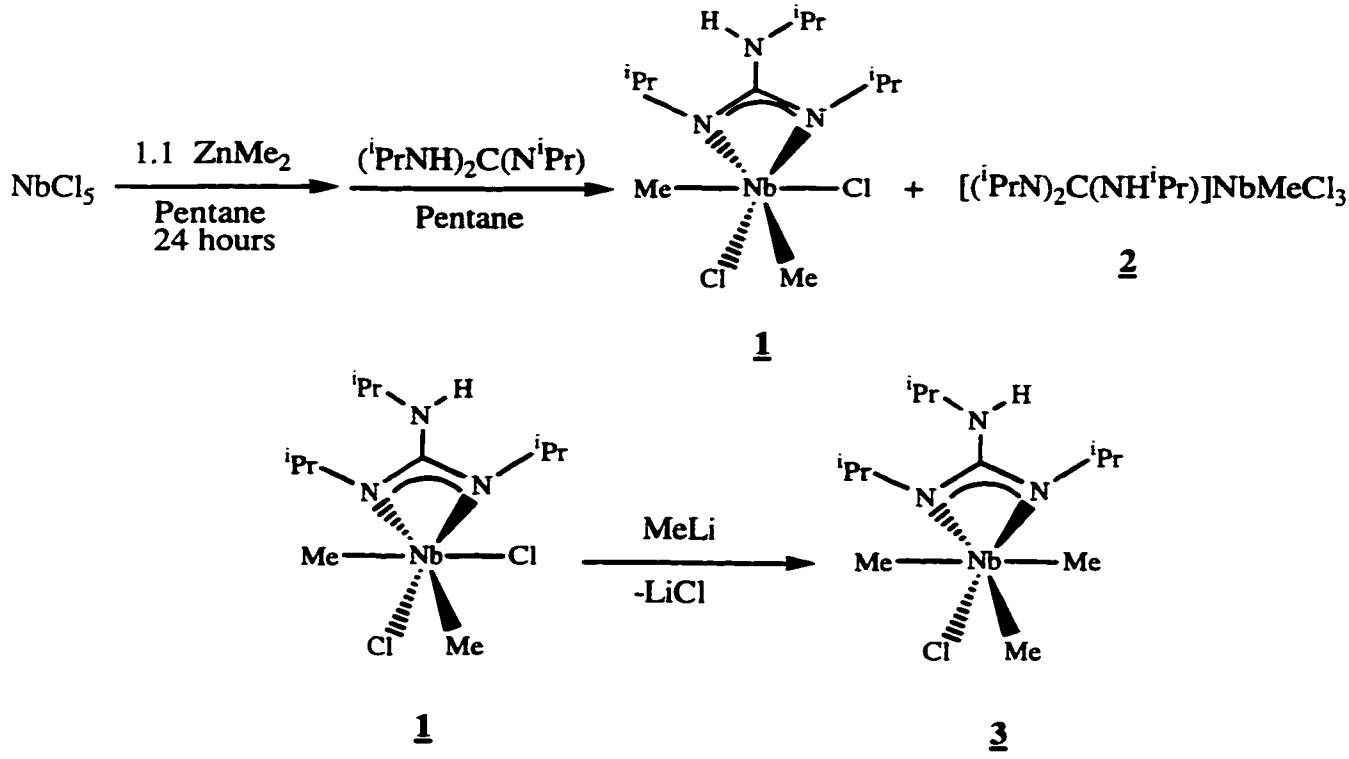

Scheme 2

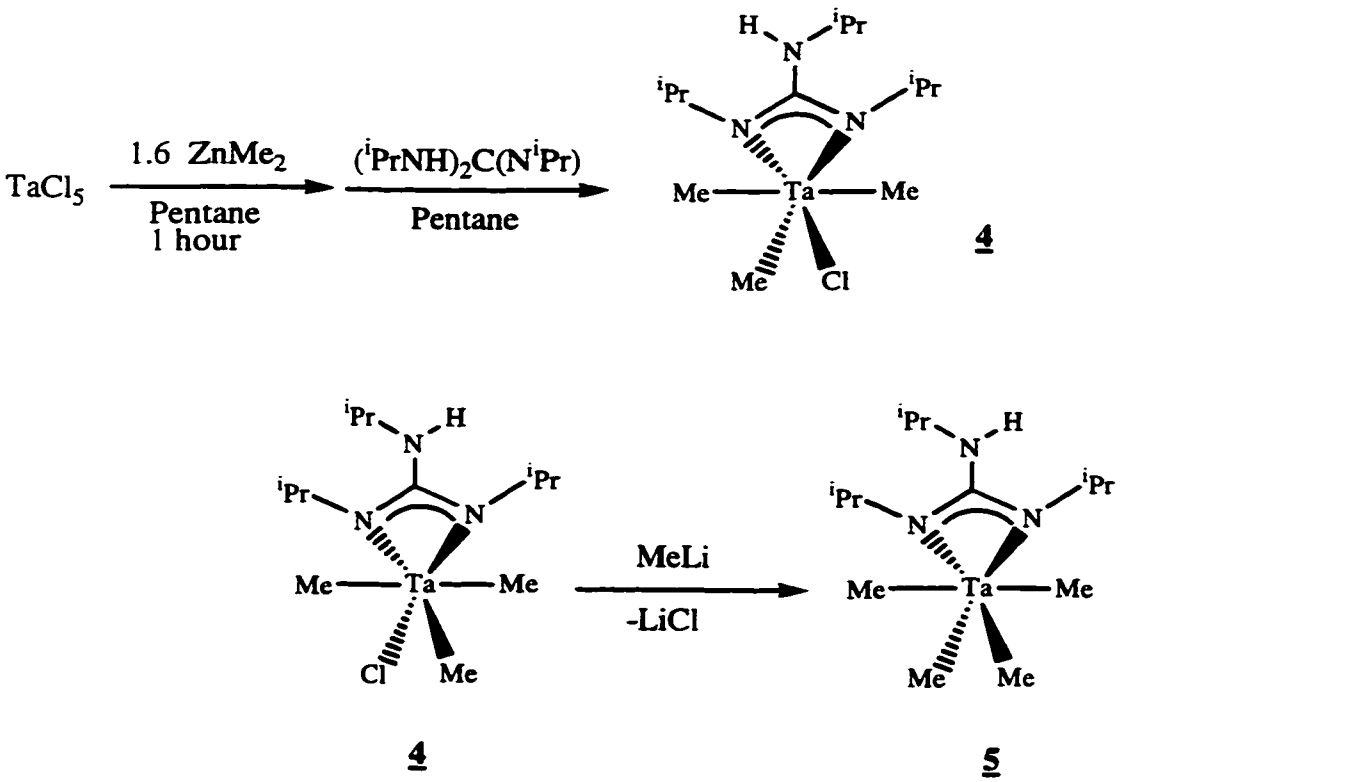

Scheme 3

Table 1. Crystal data for compounds $NbMe_2Cl_2(^iPrN)_2C(NH^iPr)$ (**1**), $NbMeCl_3\{[^iPrN]_2C[NH^iPr]\}$ (**2**), $NbMe_3Cl(^iPrN)_2C(NH^iPr)$ (**3**) and $TaMe_3Cl(^iPrN)_2C(NH^iPr)$ (**4**)

	$NbMe_2Cl_2(^iPrN)_2C(NH^iPr)$	$NbMeCl_3(^iPrN)_2C(NH^iPr)$	$TaMe_3Cl(^iPrN)_2C(NH^iPr)$	$NbMe_3Cl(^iPrN)_2C(NH^iPr)$
Empirical formula	$C_{12}H_{28}Cl_2N_3Nb$	$C_{11}H_{25}Cl_3N_3Nb$	$C_{13}H_{31}ClN_3Ta$	$C_{13}H_{31}ClN_3Nb$
Formula weight	378.18	398.60	445.81	357.77
Temperature (K)	238(2)	203(2)	203(2)	203(2)
Wavelength (Å)	0.71073	0.71073	0.71073	0.71073
Crystal system	Monoclinic	Monoclinic	Monoclinic	Monoclinic
Space group	$P2_1/c$	$P2_1/c$	$P2_1/n$	$P2_1/n$
Unit cell dimensions (Å, deg)	a = 9.309(1)	a = 9.267(1)	a = 10.536(1)	a = 10.540(2)
	b = 15.899(2)	b = 15.799(2)	b = 12.493(1)	b = 12.450(2)
	c = 12.578(2)	c = 12.646(1)	c = 13.847(1) A	c = 13.906(2)
	β = 106.492(2)	β = 106.747(2)	β = 93.058(2)	β = 92.529(3)
Volume ($Å^3$), Z	1785.0(5), 4	1772.9(3), 4	1819.9(3), 4	1823.2(5), 4
Density (Mg/m^3) (calculated)	1.407	1.493	1.627	1.303
Absorption coefficient (mm^{-1})	0.964	1.120	6.177	0.798
F(000)	784	816	880	752
Crystal size (mm)	0.4 x 0.4 x 0.4	0.1 x 0.1 x 0.02	0.1 x 0.1 x 0.1	0.2 x 0.1 x 0.02
Limiting indices	-10≤h≤9	-9≤h≤9	-14≤h≤13	-8≤h≤8
	0≤k≤17	0≤k≤17	0≤k≤16	-10≤k≤10
	0≤l≤13	0≤l≤13	0≤l≤17	-11≤l≤11
Reflections collected	13650	13958	14064	4972
Independent reflections	2320 [R(int) = 0.0581]	2313 [R(int) = 0.0959]	4314 [R(int) = 0.0530]	1141 [R(int) = 0.0896]
Absorption correction	Semi-empirical from equivalents	Semi-empirical from equivalents	Semi-empirical from equivalents	Semi-empirical from equivalents
Refinement method	Full-matrix least-squares on F^2	Full-matrix least-squares on F^2	Full-matrix least-squares on F^2	Full-matrix least-squares on F^2
Data / restraints / parameters	2320 / 0 / 165	2313 / 0 / 163	4314 / 0 / 164	1141 / 0 / 98
Goodness-of-fit on F^2	1.037	1.038	1.006	1.085
Final R indices [I>2σ(I)]	R1 = 0.0364	R1 = 0.0439	R1 = 0.0329	R1 = 0.0756
	wR2 = 0.0991	wR2 = 0.1111	wR2 = 0.0599	wR2 = 0.1982
R indices (all data)	R1 = 0.0423	R1 = 0.0638	R1 = 0.0548	R1 = 0.0875
	wR2 = 0.1017	wR2 = 0.1182	wR2 = 0.0629	wR2 = 0.2036

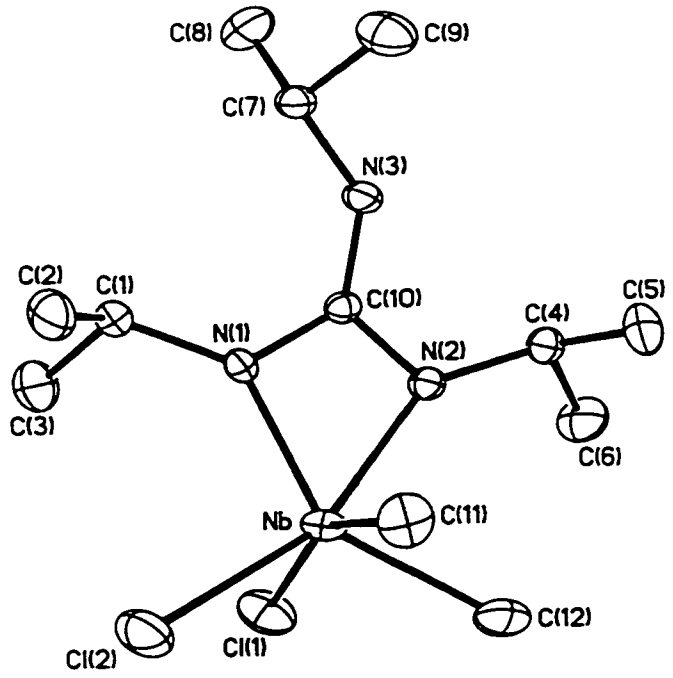

Figure 1. Molecular diagram for $NbMe_2Cl_2[(^iPrN)_2C(NH^iPr)]$ (**1**). Thermal ellipsoids are drawn at 30% probability. Hydrogen atoms have been omitted for clarity.

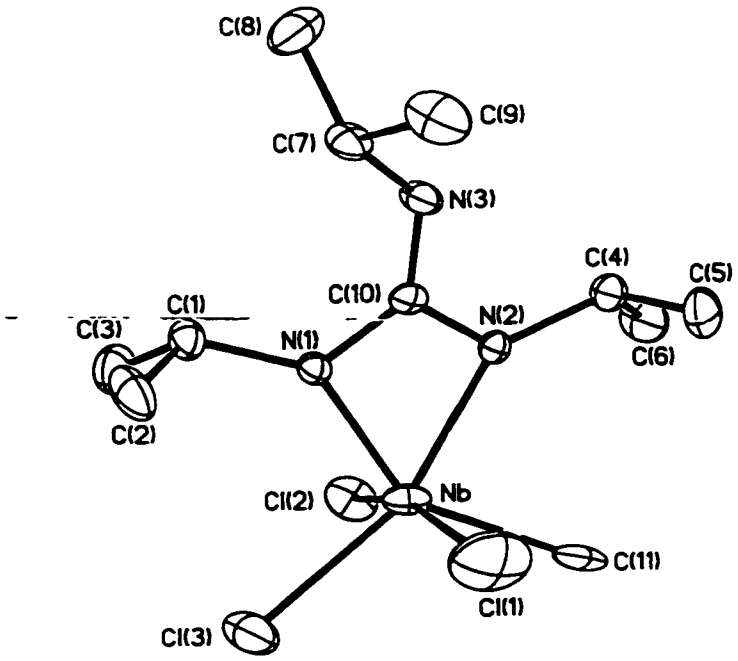

Figure 2. Molecular diagram for $NbMeCl_3[(^iPrN)_2C(NH^iPr)]$ (**2**). Thermal ellipsoids are drawn at 30% probability. Hydrogen atoms have been omitted for clarity.

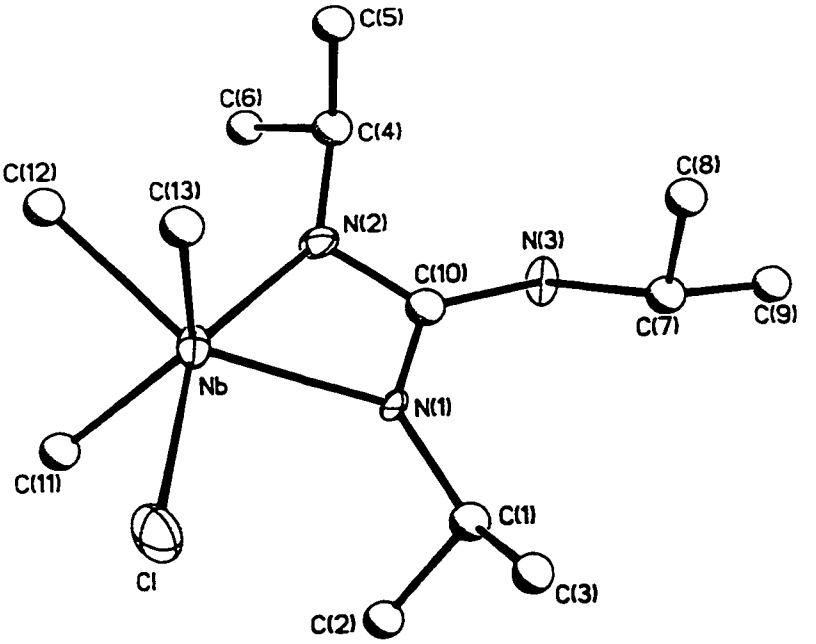

Figure 3. Molecular diagram for $NbMe_3Cl[(^iPrN)_2C(NH^iPr)]$ (**3**). Thermal ellipsoids are drawn at 30% probability. Hydrogen atoms have been omitted for clarity.

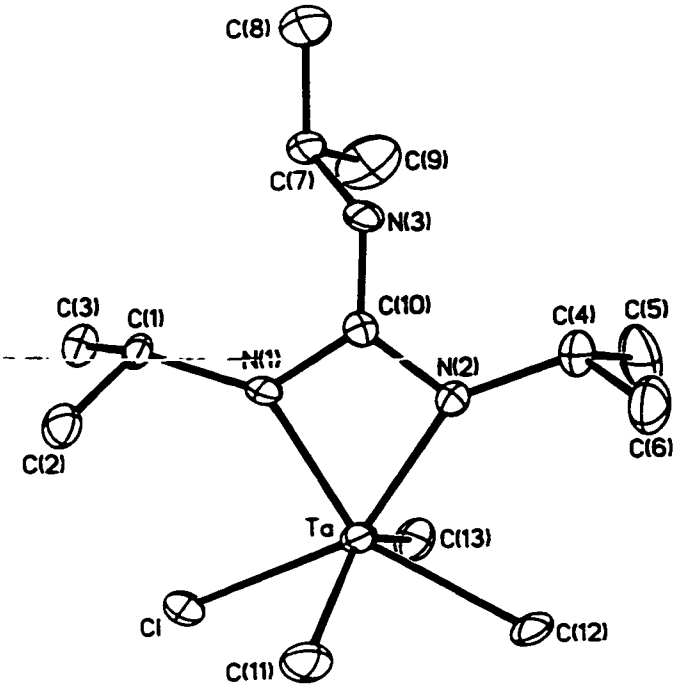

Figure 4. Molecular diagram for $TaMe_3Cl[(^iPrN)_2C(NH^iPr)]$ (**4**). Thermal ellipsoids are drawn at 30% probability. Hydrogen atoms and the 9% contribution from disorder (see text) have been omitted for clarity.

Table 2. Bond lengths [Å] and angles [deg] for $NbMe_2Cl_2[(^iPrN)_2C(NH^iPr)]$ (**1**)

Distances			
Nb-N(1)	2.050(3)	N(2)-C(4)	1.478(5)
Nb-N(2)	2.131(3)	N(3)-C(10)	1.326(5)
Nb-C(12)	2.216(5)	N(3)-C(7)	1.470(5)
Nb-C(11)	2.252(4)	C(1)-C(2)	1.523(7)
Nb-Cl(1)	2.4022(12)	C(1)-C(3)	1.526(7)
Nb-Cl(2)	2.4129(13)	C(4)-C(5)	1.503(7)
Nb-C(10)	2.577(4)	C(4)-C(6)	1.536(6)
N(1)-C(10)	1.355(5)	C(7)-C(9)	1.507(6)
N(1)-C(1)	1.476(5)	C(7)-C(8)	1.508(7)
N(2)-C(10)	1.351(5)		

Angles			
N(1)-Nb-N(2)	62.49(12)	C(10)-N(1)-Nb	96.2(2)
N(1)-Nb-C(12)	145.39(14)	C(1)-N(1)-Nb	137.3(3)
N(2)-Nb-C(12)	83.47(14)	C(10)-N(2)-C(4)	119.3(3)
N(1)-Nb-C(11)	96.32(15)	C(10)-N(2)-Nb	92.7(2)
N(2)-Nb-C(11)	96.94(15)	C(4)-N(2)-Nb	145.4(3)
C(12)-Nb-C(11)	80.94(19)	C(10)-N(3)-C(7)	129.7(3)
N(1)-Nb-Cl(1)	107.82(10)	N(1)-C(1)-C(2)	110.7(4)
N(2)-Nb-Cl(1)	101.62(9)	N(1)-C(1)-C(3)	109.8(4)
C(12)-Nb-Cl(1)	83.80(15)	C(2)-C(1)-C(3)	112.1(4)
C(11)-Nb-Cl(1)	154.40(13)	N(2)-C(4)-C(5)	112.5(4)
N(1)-Nb-Cl(2)	95.51(9)	N(2)-C(4)-C(6)	110.5(4)
N(2)-Nb-Cl(2)	157.98(9)	C(5)-C(4)-C(6)	113.0(4)
C(12)-Nb-Cl(2)	118.23(12)	N(3)-C(7)-C(9)	109.1(4)
C(11)-Nb-Cl(2)	83.85(13)	N(3)-C(7)-C(8)	109.7(4)
Cl(1)-Nb-Cl(2)	85.43(5)	C(9)-C(7)-C(8)	111.9(4)
N(1)-Nb-C(10)	31.53(12)	N(3)-C(10)-N(2)	125.1(3)
N(2)-Nb-C(10)	31.58(12)	N(3)-C(10)-N(1)	128.2(3)
C(12)-Nb-C(10)	113.89(14)	N(2)-C(10)-N(1)	106.6(3)
C(11)-Nb-C(10)	93.13(15)	N(3)-C(10)-Nb	167.2(3)
Cl(1)-Nb-C(10)	111.87(9)	N(2)-C(10)-Nb	55.70(18)
Cl(2)-Nb-C(10)	126.48(9)	N(1)-C(10)-Nb	52.28(18)
C(10)-N(1)-C(1)	125.8(3)		

Table 3. Bond lengths [Å] and angles [deg] for $NbMeCl_3[(^iPrN)_2C(NH^iPr)]$ (**2**)

Distances			
Nb-N(1)	2.041(5)	N(2)-C(4)	1.486(7)
Nb-N(2)	2.125(5)	N(3)-C(10)	1.346(7)
Nb-C(11)	2.278(7)	N(3)-C(7)	1.450(7)
Nb-Cl(1)	2.351(3)	C(1)-C(3)	1.509(9)
Nb-Cl(2)	2.3784(19)	C(1)-C(2)	1.524(10)
Nb-Cl(3)	2.416(2)	C(4)-C(6)	1.496(9)
Nb-C(10)	2.556(6)	C(4)-C(5)	1.505(9)
N(1)-C(10)	1.345(7)	C(7)-C(8)	1.500(9)
N(1)-C(1)	1.480(7)	C(7)-C(9)	1.510(9)
N(2)-C(10)	1.337(7)		

Angles			
N(1)-Nb-N(2)	62.36(18)	C(10)-N(1)-Nb	95.8(4)
N(1)-Nb-C(11)	146.4(2)	C(1)-N(1)-Nb	137.1(4)
N(2)-Nb-C(11)	84.19(19)	C(10)-N(2)-C(4)	120.5(5)
N(1)-Nb-Cl(1)	95.26(15)	C(10)-N(2)-Nb	92.3(3)
N(2)-Nb-Cl(1)	95.18(15)	C(4)-N(2)-Nb	144.7(4)
C(11)-Nb-Cl(1)	84.08(19)	C(10)-N(3)-C(7)	130.2(5)
N(1)-Nb-Cl(2)	101.99(14)	N(1)-C(1)-C(3)	110.9(5)
N(2)-Nb-Cl(2)	98.01(14)	N(1)-C(1)-C(2)	110.9(6)
C(11)-Nb-Cl(2)	84.77(18)	C(3)-C(1)-C(2)	112.5(6)
Cl(1)-Nb-Cl(2)	161.76(9)	N(2)-C(4)-C(6)	111.1(5)
N(1)-Nb-Cl(3)	96.43(14)	N(2)-C(4)-C(5)	111.5(5)
N(2)-Nb-Cl(3)	158.79(14)	C(6)-C(4)-C(5)	113.9(6)
C(11)-Nb-Cl(3)	117.01(16)	N(3)-C(7)-C(8)	109.4(6)
Cl(1)-Nb-Cl(3)	86.77(9)	N(3)-C(7)-C(9)	109.1(6)
Cl(2)-Nb-Cl(3)	85.48(7)	C(8)-C(7)-C(9)	112.4(6)
N(1)-Nb-C(10)	31.57(18)	N(2)-C(10)-N(1)	107.1(5)
N(2)-Nb-C(10)	31.51(18)	N(2)-C(10)-N(3)	124.8(5)
C(11)-Nb-C(10)	114.9(2)	N(1)-C(10)-N(3)	127.9(5)
Cl(1)-Nb-C(10)	91.09(14)	N(2)-C(10)-Nb	56.2(3)
Cl(2)-Nb-C(10)	106.71(13)	N(1)-C(10)-Nb	52.6(3)
Cl(3)-Nb-C(10)	127.52(15)	N(3)-C(10)-Nb	165.3(4)
C(10)-N(1)-C(1)	126.8(5)		

Table 4. Bond lengths [Å] and angles [deg] for $NbMe_3Cl[(^iPrN)_2C(NH^iPr)]$ (**3**).

Distances			
Nb-N(1)	2.102(9)	N(2)-C(10)	1.337(16)
Nb-N(2)	2.143(11)	N(2)-C(4)	1.491(19)
Nb-C(11)	2.155(12)	N(3)-C(10)	1.344(15)
Nb-C(13)	2.178(13)	N(3)-C(7)	1.482(15)
Nb-C(12)	2.215(12)	C(1)-C(2)	1.525(17)
Nb-Cl	2.448(4)	C(1)-C(3)	1.536(16)
Nb-C(10)	2.603(15)	C(4)-C(5)	1.444(18)
N(1)-C(10)	1.348(14)	C(4)-C(6)	1.523(18)
N(1)-C(1)	1.472(13)	C(7)-C(8)	1.470(18)
		C(7)-C(9)	1.535(17)

Angles			
N(1)-Nb-N(2)	61.7(4)	C(10)-N(1)-Nb	95.5(8)
N(1)-Nb-C(11)	111.4(4)	C(1)-N(1)-Nb	139.2(8)
N(2)-Nb-C(11)	111.1(4)	C(10)-N(2)-C(4)	119.7(12)
N(1)-Nb-C(13)	108.7(5)	C(10)-N(2)-Nb	94.0(8)
N(2)-Nb-C(13)	102.5(4)	C(4)-N(2)-Nb	143.1(10)
C(11)-Nb-C(13)	136.3(5)	C(10)-N(3)-C(7)	124.0(9)
N(1)-Nb-C(12)	145.2(4)	N(1)-C(1)-C(2)	110.3(10)
N(2)-Nb-C(12)	83.5(4)	N(1)-C(1)-C(3)	112.0(10)
C(11)-Nb-C(12)	78.2(5)	C(2)-C(1)-C(3)	110.7(10)
C(13)-Nb-C(12)	78.8(5)	C(5)-C(4)-N(2)	114.2(13)
N(1)-Nb-Cl	89.0(3)	C(5)-C(4)-C(6)	116.9(14)
N(2)-Nb-Cl	150.3(3)	N(2)-C(4)-C(6)	109.2(11)
C(11)-Nb-Cl	82.6(4)	C(8)-C(7)-N(3)	110.6(11)
C(13)-Nb-Cl	81.5(4)	C(8)-C(7)-C(9)	110.0(11)
C(12)-Nb-Cl	125.8(3)	N(3)-C(7)-C(9)	108.2(10)
N(1)-Nb-C(10)	31.0(3)	N(2)-C(10)-N(1)	108.4(12)
N(2)-Nb-C(10)	30.8(4)	N(2)-C(10)-N(3)	126.2(11)
C(11)-Nb-C(10)	117.2(4)	N(1)-C(10)-N(3)	125.2(11)
C(13)-Nb-C(10)	106.1(5)	N(2)-C(10)-Nb	55.2(7)
C(12)-Nb-C(10)	114.3(4)	N(1)-C(10)-Nb	53.5(6)
Cl-Nb-C(10)	119.6(3)	N(3)-C(10)-Nb	171.1(8)
C(10)-N(1)-C(1)	121.3(10)		

Table 5. Bond lengths [Å] and angles [deg] for $TaMe_3Cl[(^iPrN)_2C(NH^iPr)]$ (**4**)[a]

Distances			
Ta-N(1)	2.094(4)	N(2)-C(4)	1.482(5)
Ta-N(2)	2.124(4)	N(3)-C(10)	1.345(6)
Ta-C(11)	2.167(5)	N(3)-C(7)	1.478(6)
Ta-C(13)	2.172(5)	C(1)-C(3)	1.524(6)
Ta-C(12)	2.272(4)	C(1)-C(2)	1.529(6)
Ta-Cl	2.4351(13)	C(4)-C(5)	1.502(8)
Ta-C(10)	2.588(5)	C(4)-C(6)	1.503(7)
N(1)-C(10)	1.339(5)	C(7)-C(9)	1.515(8)
N(1)-C(1)	1.488(5)	C(7)-C(8)	1.519(7)
N(2)-C(10)	1.338(6)		

Angles			
N(1)-Ta-N(2)	61.76(14)	C(10)-N(1)-Ta	95.3(3)
N(1)-Ta-C(11)	109.01(18)	C(1)-N(1)-Ta	139.8(3)
N(2)-Ta-C(11)	110.45(19)	C(10)-N(2)-C(4)	120.4(4)
N(1)-Ta-C(13)	108.32(18)	C(10)-N(2)-Ta	94.0(3)
N(2)-Ta-C(13)	103.58(18)	C(4)-N(2)-Ta	142.1(3)
C(11)-Ta-C(13)	138.1(2)	C(10)-N(3)-C(7)	125.0(4)
N(1)-Ta-C(12)	146.21(15)	N(1)-C(1)-C(3)	112.6(4)
N(2)-Ta-C(12)	84.55(14)	N(1)-C(1)-C(2)	110.4(4)
C(11)-Ta-C(12)	78.97(18)	C(3)-C(1)-C(2)	111.0(4)
C(13)-Ta-C(12)	80.64(17)	N(2)-C(4)-C(5)	112.9(5)
N(1)-Ta-Cl	87.63(10)	N(2)-C(4)-C(6)	111.3(5)
N(2)-Ta-Cl	149.08(10)	C(5)-C(4)-C(6)	114.9(5)
C(11)-Ta-Cl	82.33(16)	N(3)-C(7)-C(9)	110.1(4)
C(13)-Ta-Cl	80.79(15)	N(3)-C(7)-C(8)	109.0(4)
C(12)-Ta-Cl	126.15(11)	C(9)-C(7)-C(8)	111.9(5)
N(1)-Ta-C(10)	31.02(13)	N(2)-C(10)-N(1)	107.9(4)
N(2)-Ta-C(10)	31.05(13)	N(2)-C(10)-N(3)	126.5(4)
C(11)-Ta-C(10)	116.45(18)	N(1)-C(10)-N(3)	125.6(4)
C(13)-Ta-C(10)	105.37(18)	N(2)-C(10)-Ta	55.0(2)
C(12)-Ta-C(10)	115.54(15)	N(1)-C(10)-Ta	53.7(2)
Cl-Ta-C(10)	118.04(10)	N(3)-C(10)-Ta	172.1(3)
C(10)-N(1)-C(1)	122.0(4)		

[a] The values in Table 5 represent those for modeled disorder between the Cl and C(12) sites. See text for description.

A small amount of a second compound crystallized during the preparation of **1**. Single crystals of this material were obtained and an x-ray diffraction study was performed. Complex **2** Scheme 2 has pseudo-octahedral coordination geometry consisting of a monoanionic triisopropylguanidinate ligand, one Nb-Me function and three chloro ligands. The equatorial plane is defined by N(1), N(2), C(11), and Cl(3) (sum of appropriate angles = 360°) with the guanidinate displaying a bite angle N(1)-Nb-N(2) of 62.36(18)°. Two chloro ligands, Cl(1) and Cl(2), can be placed along the pseudo-axial direction the observed Cl(1)-Nb-Cl(2) angle was 161.76(9)° with these two ligands are bent toward the Cl(3)-Nb-C(11) angle. This distortion does not appear to be due to steric factors. The guanidinate C(10)-N(1) (1.345(7)Å) and N(2)-C(10) (1.337(7)Å) distances are consistent with partial double bond character for this moiety.

The third guanidinate nitrogen atom, N(3), lies outside of the metal coordination sphere but is nearly co-planar with the M-N-C-N plane [N(3)-C(10)-Nb angle of 165.3(4)°]. The only measurable angle around N(3) (C(10)-N(3)-C(7) = 130.2(5)°) is consistent with assignment of an sp^2 nitrogen. A small dihedral angle of 19.0° between the mean planes defined by atoms bonded to N(3) and the N(1)-C(10)-N(2) group would allow for conjugation of a p orbital localized lone pair on N(3) with the π system of the coordinated atoms. Further evidence for the contribution of the zwitterionic form (**II**, scheme 1) is provided by relatively short C(10)-N(3) distance of 1.346(7)Å compared to the three N-C(isopropyl) bonds (N(1)-C(1), N(2)-C(4), N(3)-C(7)) which average 1.47Å. However, free rotation about the C(10)-N(3) bond is observed in the ^1H and ^{13}C NMR spectra of **2** and is contradictory to a strong π interaction between these two atoms.

Conclusive confirmation of the identity of **4** is provided from the results of x-ray diffraction analyses. Examination of Figure 4 confirms the ^1H NMR results and shows that **4**

does indeed possess three methyl groups (one more than initially anticipated). A bidentate guanidinate monoanion (bite angle of 61.76(14)°), three Me groups, and one Cl ligand make up the coordination sphere for a distorted pseudo-octahedral Ta center. The equatorial plane is defined by N(1), N(2), C(12), and Cl with C(13) and C(11) lying along the pseudo-axial vector. Obtaining precise values for bond distances and angles in **4** was hampered by the fact that the chloride ligand Cl and C(12) were found to be disordered over these two positions in a 91:9 ratio.

As noted for **1** and **2**, the C(13)TaC(11) angle which defines the pseudo axial directions in **4** is disordered [138.1(2)°] such that the two axial ligands are bent toward the ClTaC(12) angle. Based on this small number of compounds a decrease in the angle defined by the axial ligands seems to follow with increased degree of alkylation of the metal center. The C(7)-N(3)-C(10) angle of 125.0(4)° is in line with the observations in all of these complexes as are the N(1)-C(10), N(3)-C(10) and N(3)-C(10) distances of 1.339(5)Å, 1.338(6)Å and 1.345(6) Å respectively. In this case the dihedral angle formed between the mean planes defined by C(10)-N(3)-C(7) and N(1)-C(10)-N(2) is quite a bit larger than was observed for **1** and **2** having a value of 41.7°.

Complexes **1** and **4** are susceptible to methylation by MeLi to give complexes with three and four methyl ligands respectively. These metathesis reactions proceed smoothly and in good yield. NMR spectroscopic characterization indicated that these reactions proceeded according to Schemes 2 and 3 to yield complexes **3** and **5**.

Confirmation of the identity and structural features for **3** was obtained by single crystal x-ray analysis. Given the analogy of **3** with **4** a comparison of Figures 3 and 4 of the structural parameters of these two complexes (Tables 4 and 5) is appropriate. The gross structural features of these two species are very similar. For example the axial methyl groups,

C(11) and C(13), are nearly symmetrically disposed above and below the equatorial plane defined by the guanidinate ligand, C(12) and Cl with a C(11)-Nb-C(13) angle of 136.3(5)°. A trend in axial preference for methylation and a decrease of the axial ligand-M-axial ligand angle is systematically observed for all of the structurally characterized species. The planar metal containing cycle formed by the guanidinate ligand with a bite angle of 61.7(4)° as well as the structural parameters associated with N(1), N(2) and N(3) are again similar to **4** and the other complexes reported herein.

Interestingly, methylation of the metal center also seems to lead to a larger dihedral angle between the plane of the non coordinated nitrogen center C(10)-N(3)-C(7) and the N(1)-C(10)-N(2) plane. For example, the two trimethyl complexes, **3** and **4**, exhibited the largest values for this parameter with essentially equal angles of 41.6° and 41.7° respectively. This effect leads to reduced π overlap within the ligand which would be necessary to form a fully conjugated system containing a dianionic guanidinate ligand.

Based on the fact that Me_4TaCl is not accessible from the reaction of $ZnMe_2$ with Me_3TaCl_2 and the fact that MMe_xCl_{5-x} (M = Nb, x = 2; M = Ta, x = 3) are well documented species in the literature,[3] we speculate that species **1** and **4** originate from elimination of HCl from the starting alkyls. Preliminary ^1H NMR and mass spectroscopy data of an authentic sample of hydrochloric guanidinium salt is in agreement with ^1H NMR and mass spectroscopy data of the by-product solid produced during the making of species **1** and **4**.

Methylation of these species can be performed by the addition of one equivalent of MeLi to either **1** or **4** to generate **3** and **5** (Scheme 2 and 3). These reactions proceed smoothly and quickly with no visible bubbling which would indicate the MeLi had reacted with the guanidines N-H function instead of the M-Cl function.

Efforts to get the elimination of a second methyl group and generation of the coordinated guanidinate dianion were performed. Probably the most obvious choice is to heat these compounds and see if this thermal energy is enough to drive the complexes to reductively eliminate a methane molecule. Unfortunately these compounds are very temperature sensitive and judging by the NMR spectra gave decomposition upon heating. Another attempt involved the addition of lithium dimethyl amide to complex **4**. This reaction was exceedingly fast even at low temperatures and yielded an orange oil. The NMR spectra were very complicated and suggested that many products were formed during this reaction. Purification attempts of subsequent reactions to obtain the dianion have all been unsuccessful as yet.

References

(1) Snaith, R.; Wade, K.; Wyatt, B. K. *J. Chem. Soc. (A)* **1970**, 380

(2) Tin M.K.T.; Yap G. P. A.; Richeson D. S. *Inorg. Chem.* **1998**, 37, 6728

(3) Shrock, R. R.; Parshall, G. W. *Chem. Rev.* **1976**, 76, 243

(4) Tin M.K.T.; Thirupathi N.; Yap G. P. A.; Richeson D. S. *J. Chem. Soc., Dalton Trans.* **1999**, 2947

Chapter 4

Triisopropylguanidinate Anions and Dianions As Supporting Ligands for Zirconium Monomers and Dimers

Introduction

This chapter combines the methods developed in chapters 2 and 3 for the introduction of guanidinates into the coordination sphere of some Zr(IV) complexes, specifically deprotonation/elimination reactions and metathesis reactions are employed.

To date, Group 4 metallocenes (**I**, Scheme 1)[1] and the related catalyst systems such as the half sandwich amides (**II**, Scheme 1 - "constrained geometry catalysts") have been important in increasing the understanding of the factors that are important for stabilizing polymerization active metal centers and controlling their activity and selectivity. Our efforts in this realm involve the possibility of employing triisopropyl guanidine as a substitute for the important Cp ligand in order to generate Cp free catalytic systems. The variety of coordination modes available to guanidines combined with the ability to tune the sterics of the ligand system by changing the size of the organic substituents provides for a flexible system for study.

There is only one reported group of guanidinate complexes of group 4 which was prepared by the reaction of $M(NMe_2)_4$ with di(p-tolyl)carbodiimide (M = Ti) or with dicyclohexylcarbodiimide (M = Ti, Zr, Hf) giving the tetrasubstituted guanidinate complexes in good yield (Equation 4, chapter 1).[2] Further insertions of carbodiimide were prevented due to steric congestion and no attempts were made to prepare the mono insertion product.

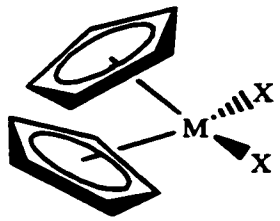

M = Ti, Zr, Hf
X = Halogen

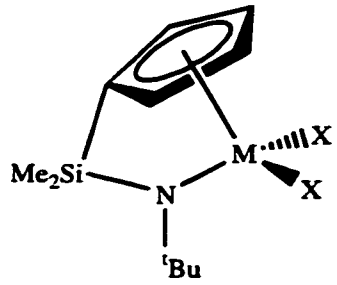

I II

Scheme 1

Experimental

General Considerations

All manipulations were carried out in either a nitrogen filled drybox or under nitrogen using standard Schlenk-line techniques. $ZrCl_4$ was used as received from Aldrich Chemical Company. Solvents were distilled under nitrogen from Na/K alloy. ^1H and ^{13}C NMR spectra were run on a Gemini 200 MHz spectrometer with C_6D_6 or $CDCl_3$ as a solvent and internal standard. $ZrBz_4$ was prepared using literature procedures.[3] All elemental analyses were run on a Perkin Elmer PE CHN 4000 elemental analysis system.

$Bz_2Zr\{(^iPrN)_2C(NH^iPr)\}_2$ (1)

To an orange solution of $ZrBz_4$ (0.173 g, 0.380 mmol) dissolved in 2-ml dichloromethane was added a colorless 2-ml dichloromethane solution of triisopropyl guanidine (0.146 g, 0.788 mmol). An immediate color change to clear yellow was observed. The mixture was allowed to sit at room temperature undisturbed for 72 hours. The solvent

was then removed to give a light yellow solid (0.214 g, 88% yield). Yellow crystals of **1** were obtained from diethylether at –35 °C.

^{1}H NMR (C_6D_6): 0.90 (m, 12H, CH_3), 1.13 (d, 24H, CH_3), 2.67 (s, 4H, CH_2), 3.48 (br, 4H, CH and NH), 3.64 (sept, 4H, CH), 6.92 (t, 1H, C_6H_5), 7.26 (t, 2H, C_6H_5), 7.45 (d, 2H, C_6H_5)

^{13}C NMR (C_6D_6): 24.6, 24.8 (2s, ***C***H_3), 46.3, 46.8 (2s, ***C***H), 70.9 (s, ***C***H_2), 119.8, 127.4, 128.2, 150.7 (4s, ***C***$_6H_5$), 168.6 (s, ***C***N_3)

EA: Calculated for $ZrN_6C_{34}H_{58}$: C 63.60; H 9.11; N 13.09. Found: C 59.20; H 8.96; N 13.50

$Cl_3Zr\{(^iPrN)_2C(NH^iPr)\}$ (2)

Toluene (75-ml) was added to the combined solids of $ZrCl_4$ (1.000 g, 4.29 mmol) and triisopropyl guanidine (1.590 g, 8.58 mmol). The resulting mixture was allowed to stir for 24 hours. Filtration gave a fluffy white solid (2.05 g), which contained compounds **2** and **3**. Repeated extraction of this solid with toluene gave a sufficient amount of soluble material of **2** to perform an NMR study.

^{1}H NMR (C_6D_6): 3.52 (broad, 4H, CH and NH), 1.45 (d, 12H, CH_3), 0.83 (d, 6H, CH_3)

^{13}C NMR (C_6D_6): 148.67 (s, ***C***N_3), 47.40 (s, ***C***H), 46.71 (s, ***C***H), 24.64 (s, ***C***H_3), 24.30 (s, ***C***H_3)

$(^iPrNH)_3CCl$ (3)

^{1}H NMR ($CDCl_3$): 7.04 (d, 3H, NH), 3.80 (sept, 3H, CH), 1.31 (d, 18H, CH_3)

$BzClZr\{(^iPrN)_2C(NH^iPr)\}_2$ (4)

To the mixture of **2** and **3** (2.05 g) in 20-ml toluene, BzMgCl (13 ml, 1M in toluene) was added. The mixture was allowed to stir for 2 hours. Filtration, concentration and cooling of filtrate to –35 °C gave yellow-green crystals of **4** (0.50 g)

^1H NMR (C_6D_6): 7.47-6.83 (m, C_6H_5, 5H), 3.71-3.39 (br, CH and NH, 8H), 2.87 (s, CH_2, 2H), 1.38-0.82 (m, CH_3, 36H)

^{13}C NMR (C_6D_6): 167.7 (s, ***C***N_3), 148.8, 129.0, 128.2, 120.4 (4s, ***C***$_6H_5$), 69.5 (s, ***C***H_2), 47.0, 46.5 (2s, ***C***H), 24.9, 24.7, 24.3 (3s, ***C***H_3)

EA: Calculated for $C_{27}H_{51}N_6ClZr$: C 55.30; H 8.77; N 14.33. Found: C 52.11; H 8.79; N 14.09

$[Cl_2Zr\{(^iPrN)_3C\}]_2$ (6)

Triisopropyl guanidine (0.500 g, 2.7 mmol) was dissolved in 40-ml diethyl ether. To this was added MeLi (3.8 ml, 1.4M in diethyl ether). The bubbling mixture was allowed to stir for an hour and then $ZrCl_4$ (0.629 g, 2.7 mmol) was added and stirred for 16 hours. Filtration and removal of the solvent from the light orange filtrate gave a yellow-orange solid (0.540 g, 58% yield). Colorless crystals of **6** could be obtained from CH_2Cl_2 at - 35 °C.

^1H NMR (C_6D_6): 4.21 (sept, 1H, CH), 3.82 (m, 2H, CH), 1.51, 1.40, 1.10 (3d, 18H, CH_3)

^{13}C NMR (C_6D_6): 165.09 (s, ***C***N_3), 60.02, 49.46 (2s, ***C***H), 27.48, 25.19, 23.19 (3s, ***C***H_3)

EA: This compound reacts too fast in air to perform elemental analysis

Results and Discussion

Three general synthetic procedures were explored for introduction of triisopropyl guanidinate into the zirconium coordination sphere, which are summarized in Equations 1-4. Equation 1 utilizes the reaction of the zirconium benzyl with active N-H function of the guanidine. Equations 2 and 3 are elimination reactions of HCl and LiCl respectively.

Spectroscopic characterization provided the first confirmation of the identity of these materials **1-6**. Compound **1** exhibited ^{1}H and ^{13}C NMR spectra with the most notable features being the appearance of two equivalent monoanionic guanidine ligands indicated by two doublets in a characteristic 2:1 ratio for the CH_3 groups on isopropyl as well as the presence of a single N-H peak. The benzyl peak appears as one singlet suggesting both benzyl groups are equivalent and that no η^2 bonding was present.

Compound **1** was analyzed by single crystal x-ray diffraction with the results presented in Figure 1 and Tables 1 and 2. The two guanidinate ligands span axial/equatorial positions with N(1) and N(4) can be placed along the axial positions [N(1)ZrN(5) angle of 155.87(5)°] of the distorted octahedral complex giving an approximate C_2 symmetric complex. The corresponding nitrogens N(2) and N(5) of the bidentate guanidine ligands make up one half of the equatorial plane while the two equatorial benzyl groups complete the coordination sphere.

$$ZrCl_4 + 4\,BzMgCl \xrightarrow{-4\,MgCl_2} ZrBz_4$$

$$ZrBz_4 + x\ (^iPrNH)_2C(N^iPr) \xrightarrow{-2\ Toluene} \textbf{1} \qquad (1)$$

x = any number

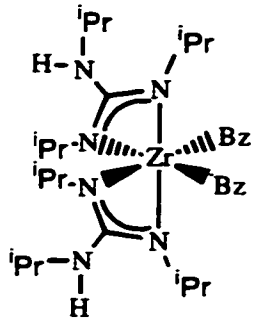

1

$$ZrCl_4 + 2\ (^iPrNH)_2C(N^iPr) \longrightarrow Cl_3Zr\{(^iPrN)_2C(NH^iPr)\} + (^iPrNH)_3CCl \qquad (2)$$

2 **3**

$$Cl_3Zr\{(^iPrN)_2C(NH^iPr)\} + (^iPrNH)_3CCl \xrightarrow{3\ BzMgCl} \textbf{4} \qquad (3)$$

2 **3**

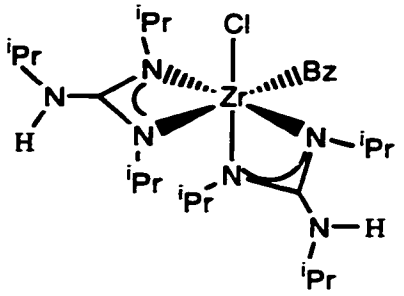

4

$$(^iPrNH)_2C(N^iPr) + 2\ MeLi \longrightarrow (^iPrN)_3CLi_2 + 2\ MeH$$

5

$$(^iPrN)_3CLi_2 + ZrCl_4 \xrightarrow{-2\ LiCl} 1/2 \qquad (4)$$

5

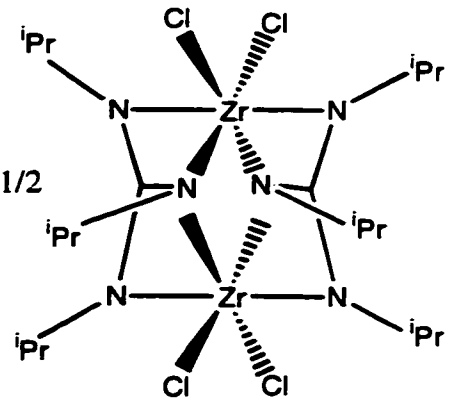

6

Table 1. Crystal data for compounds $Bz_2Zr\{(^iPrN)_2C(NH^iPr)\}_2$ (1), $BzClZr\{(^iPrN)_2C(NH^iPr)\}_2$ (4), and $[Cl_2Zr\{(^iPrN)_3C\}]_2$ (6).

Empirical formula	$C_{27}H_{51}ClN_6Zr$	$C_{34}H_{58}N_6Zr$	$C_{20}H_{42}Cl_4N_6Zr_2$
Formula weight	586.41	642.08	690.84
Temperature K	238(2) K	203(2)	203(2)
Wavelength Å	0.71073 Å	0.71073	0.71073
Crystal system, space group	Orthorhombic, Pbca	Monoclinic, $P2_1/n$	Monoclinic, $P2_1/n$
Unit cell dimensions			
a Å, α °	18.657(3), 90	10.403(1), 90	9.554(2), 90
b Å, β °	11.057(2), 90	15.202(2), 96.773(2)	14.951(3), 96.60(2)
c Å, γ °	30.086(5), 90	22.625(3), 90	10.538(2), 90
Volume $Å^3$	6206(2)	3553.1(7)	1495.4(5)
Z, Calculated density Mg/m^3	8, 1.255	4,1.200	2,1.534
Absorption coefficient mm^{-1}	0.465	0.339	1.073
F(000)	2496	1376	704
Crystal size mm	0.2 x 0.2 x 0.2	0.30x0.30x0.10	0.1x0.1x0.08 mm
θ range for data collection °	2.25 to 26.38	1.62 to 28.27	2.38 to 21.00
Limiting indices	$0\le h\le 23$, $0\le k\le 13$, $0\le l\le 37$	$-13\le h\le 13$, $0\le k\le 19$, $0\le l\le 29$	$-9\le h\le 9$, $-10\le k\le 15$, $-10\le l\le 10$
Reflections collected/unique	48810/6341 [R(int) = 0.10761	8566/8266 [R(int)=0.0354]	4166/1554 [R(int)=0.1386]
Absorption correction	Semi-empirical from equivalents	None	Semi-empirical from equivalents
Max. and min. transmission	0.928076 and 0.726339	0.9669 and 0.9050	0.526414 and 0.188298
Refinement method	Full-matrix least-squares on F^2	Full-matrix least-squares on F^2	Full-matrix least-squares on F^2
Data/restraints/parameters	6341/0/316	8266/0/370	1554/24/145
Goodness-of-fit on F^2	1.047	1.063	1.005
Final R indices [$I>2\sigma(I)$]	R1=0.0333, wR2=0.0661	R1=0.0324, wR2=0.0874	R1=0.0472, wR2=0.0924
R indices (all data)	R1=0.0646, wR2=0.0706	R1=0.0403, wR2=0.0891	R1=0.0975, wR2=0.1177

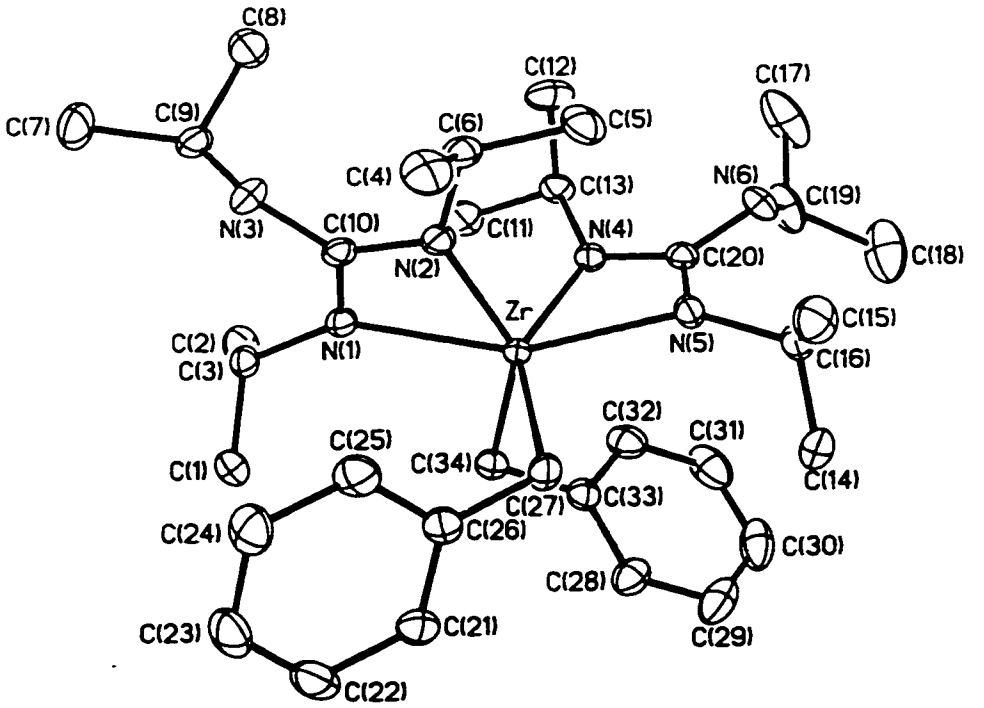

Figure 1.Molecular diagram for $Bz_2Zr[(^iPrN)_2C(NH^iPr)]_2$ (**1**). Thermal ellipsoids are drawn at 30% probability. Hydrogen atoms have been omitted for clarity.

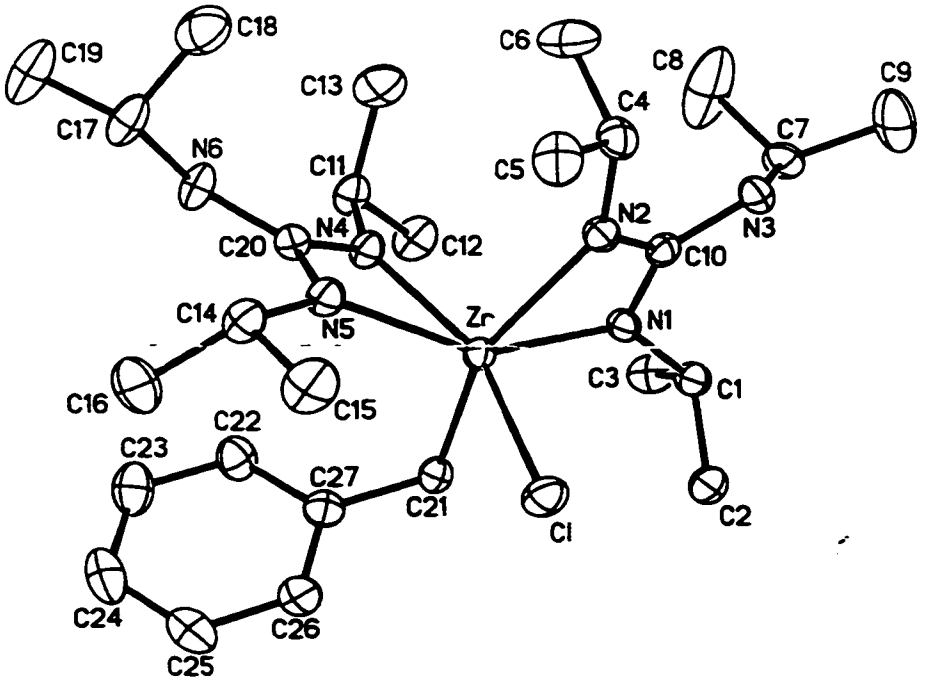

Figure 2. Molecular diagram for $BzClZr[(^iPrN)_2C(NH^iPr)]_2$ (**4**). Thermal ellipsoids are drawn at 30% probability. Hydrogen atoms have been omitted for clarity.

Table 2. Bond distances and angles for $Bz_2Zr[(^iPrN)_2C(NH^iPr)]_2$ (**1**)

Bond distances					
Zr-N(4)	2.1873(14)	Zr-N(2)	2.2091(14)	N(5)-C(20)	1.330(2)
Zr-N(1)	2.2918(14)	Zr-N(5)	2.2925(14)	N(6)-C(20)	1.372(2)
Zr-C(34)	2.3162(17)	Zr-C(27)	2.3176(17)	C(26)-C(27)	1.467(2)
Zr-C(20)	2.6946(16)	Zr-C(10)	2.7006(16)	N(5)-C(16)	1.482(2)
N(1)-C(10)	1.328(2)	N(1)-C(3)	1.475(2)	N(6)-C(19)	1.476(2)
N(2)-C(10)	1.347(2)	N(2)-C(6)	1.467(2)	C(33)-C(34)	1.480(2)
N(3)-C(10)	1.380(2)	N(3)-C(9)	1.477(2)		
N(4)-C(20)	1.347(2)	N(4)-C(13)	1.473(2)		
Bond angles					
N(4)-Zr-N(2)	98.89(5)	C(3)-N(1)-Zr	144.35(11)	N(6)-C(19)-C(18)	108.5(2)
N(4)-Zr-N(1)	105.92(5)	C(10)-N(2)-C(6)	121.44(14)	N(6)-C(19)-C(17)	111.6(2)
N(2)-Zr-N(1)	59.16(5)	C(10)-N(2)-Zr	95.77(10)	N(5)-C(20)-N(4)	111.95(14)
N(4)-Zr-N(5)	59.31(5)	C(6)-N(2)-Zr	141.43(11)	N(5)-C(20)-N(6)	124.78(16)
N(2)-Zr-N(5)	102.05(5)	C(10)-N(3)-C(9)	122.33(15)	N(4)-C(20)-N(6)	123.24(16)
N(1)-Zr-N(5)	155.87(5)	C(20)-N(4)-C(13)	123.28(14)	N(5)-C(20)-Zr	58.22(9)
N(4)-Zr-C(34)	93.52(6)	C(20)-N(4)-Zr	96.45(10)	N(4)-C(20)-Zr	53.76(8)
N(2)-Zr-C(34)	144.81(6)	C(13)-N(4)-Zr	135.71(11)	N(6)-C(20)-Zr	175.52(13)
N(1)-Zr-C(34)	85.81(6)	C(20)-N(5)-C(16)	120.74(14)	C(26)-C(27)-Zr	113.21(11)
N(5)-Zr-C(34)	112.56(6)	C(20)-N(5)-Zr	92.24(10)	C(33)-C(34)-Zr	111.24(11)
N(4)-Zr-C(27)	144.34(6)	C(16)-N(5)-Zr	144.72(11)	N(5)-Zr-C(10)	129.98(5)
N(2)-Zr-C(27)	95.96(6)	C(20)-N(6)-C(19)	123.25(16)	C(34)-Zr-C(10)	115.22(6)
N(1)-Zr-C(27)	109.55(6)	N(1)-C(3)-C(1)	111.19(15)	C(27)-Zr-C(10)	105.49(6)
N(5)-Zr-C(27)	85.97(6)	N(1)-C(3)-C(2)	112.14(15)	C(20)-Zr-C(10)	119.68(5)
C(34)-Zr-C(27)	92.67(7)	N(2)-C(6)-C(4)	111.46(16)	C(10)-N(1)-C(3)	120.66(14)
N(4)-Zr-C(20)	29.78(5)	N(2)-C(6)-C(5)	110.31(15)	C(10)-N(1)-Zr	92.61(10)
N(2)-Zr-C(20)	101.39(5)	N(3)-C(9)-C(7)	109.04(18)	N(4)-C(13)-C(11)	108.56(14)
N(1)-Zr-C(20)	132.85(5)	N(3)-C(9)-C(8)	110.54(16)	N(4)-C(13)-C(12)	112.05(16)
N(5)-Zr-C(20)	29.54(5)	N(1)-C(10)-N(2)	112.38(14)	N(5)-C(16)-C(14)	110.81(16)
C(34)-Zr-C(20)	105.52(6)	N(1)-C(10)-N(3)	124.98(15)	N(5)-C(16)-C(15)	111.75(17)
C(27)-Zr-C(20)	115.27(6)	N(2)-C(10)-N(3)	122.61(15)	N(1)-Zr-C(10)	29.42(5)
N(4)-Zr-C(10)	103.43(5)	N(1)-C(10)-Zr	57.97(8)	N(3)-C(10)-Zr	176.96(13)
N(2)-Zr-C(10)	29.75(5)	N(2)-C(10)-Zr	54.48(8)		

Table 3. Bond distances and angles for $BzClZr[(^{i}PrN)_2C(NH^{i}Pr)]_2$ (**4**)

Bond distances			
Zr-N(4)	2.1797(19)	N(2)-C(10)	1.338(3)
Zr-N(2)	2.2190(19)	N(2)-C(4)	1.471(3)
Zr-N(1)	2.2391(19)	N(3)-C(10)	1.372(3)
Zr-N(5)	2.2402(19)	N(3)-C(7)	1.471(3)
Zr-C(21)	2.331(2)	N(4)-C(20)	1.354(3)
Zr-Cl	2.4744(7)	N(4)-C(11)	1.468(3)
Zr-C(20)	2.658(3)	N(5)-C(20)	1.333(3)
Zr-C(10)	2.691(2)	N(5)-C(14)	1.479(3)
N(1)-C(10)	1.345(3)	N(6)-C(20)	1.365(3)
N(1)-C(1)	1.477(3)	N(6)-C(17)	1.481(3)
Bond Angles			
N(4)-Zr-N(2)	96.70(7)	N(2)-C(10)-N(1)	111.2(2)
N(4)-Zr-N(1)	101.41(7)	N(2)-C(10)-N(3)	123.4(2)
N(2)-Zr-N(1)	59.56(7)	N(1)-C(10)-N(3)	125.3(2)
N(4)-Zr-N(5)	60.56(7)	N(2)-C(10)-Zr	55.21(12)
N(2)-Zr-N(5)	98.47(7)	N(1)-C(10)-Zr	56.10(12)
N(1)-Zr-N(5)	151.42(7)	N(3)-C(10)-Zr	178.41(18)
N(4)-Zr-C(21)	91.01(8)	N(4)-C(11)-C(12)	110.0(2)
N(2)-Zr-C(21)	147.49(8)	N(4)-C(11)-C(13)	112.1(2)
N(1)-Zr-C(21)	87.97(8)	N(5)-C(14)-C(15)	110.9(2)
N(5)-Zr-C(21)	112.70(8)	N(5)-C(14)-C(16)	111.7(2)
N(4)-Zr-Cl	157.12(6)	N(6)-C(17)-C(19)	107.0(2)
N(2)-Zr-Cl	94.59(6)	N(6)-C(17)-C(18)	110.7(2)
N(1)-Zr-Cl	101.47(6)	N(5)-C(20)-N(4)	112.1(2)
N(5)-Zr-Cl	98.13(5)	N(5)-C(20)-N(6)	127.6(2)
C(21)-Zr-Cl	90.08(7)	N(4)-C(20)-N(6)	120.3(2)
N(4)-Zr-C(20)	30.52(7)	N(5)-C(20)-Zr	57.34(12)
N(2)-Zr-C(20)	99.33(7)	N(4)-C(20)-Zr	54.81(12)
N(1)-Zr-C(20)	129.00(7)	N(6)-C(20)-Zr	174.00(18)
N(5)-Zr-C(20)	30.05(7)	C(27)-C(21)-Zr	105.31(16)
C(21)-Zr-C(20)	103.11(8)	C(20)-N(6)-C(17)	128.5(2)
Cl-Zr-C(20)	127.64(6)	N(1)-C(1)-C(3)	111.2(2)
N(4)-Zr-C(10)	99.37(7)	N(1)-C(1)-C(2)	111.0(2)
N(2)-Zr-C(10)	29.69(7)	C(10)-N(3)-C(7)	125.6(2)
N(1)-Zr-C(10)	29.90(7)	C(20)-N(4)-C(11)	121.4(2)
N(5)-Zr-C(10)	125.67(7)	C(20)-N(4)-Zr	94.67(15)
C(21)-Zr-C(10)	117.88(8)	C(11)-N(4)-Zr	143.76(16)
Cl-Zr-C(10)	100.29(5)	C(20)-N(5)-C(14)	122.5(2)
C(20)-Zr-C(10)	116.16(7)	C(20)-N(5)-Zr	92.61(14)
C(10)-N(1)-C(1)	120.6(2)	C(14)-N(5)-Zr	142.68(16)
C(10)-N(1)-Zr	94.00(14)	N(2)-C(4)-C(6)	112.0(2)
C(1)-N(1)-Zr	139.27(15)	N(2)-C(4)-C(5)	108.7(2)
C(10)-N(2)-C(4)	122.4(2)	C(4)-N(2)-Zr	140.75(16)
C(10)-N(2)-Zr	95.10(14)	N(3)-C(7)-C(8)	112.0(2)
N(3)-C(7)-C(9)	109.9(2)		

The apparent equivalence of the ^{i}Pr groups bonded to N(1) and N(5) with those on N(2) and N(4) in the NMR spectra of **1** suggests that this complex is fluxional in solution. X-ray analysis confirmed the lack of η^2 bonding (of the benzyl groups) provided by NMR studies. The only measurable angles about N(3) [122.33(15)°] and N(6) [123.25(16)°] are consistent with sp^2 hybridized nitrogen atoms.

The N(4)ZrN(5) bite angle [59.31(5)°] is the same within error when compared to the N(1)ZrN(2) bite angle [59.16(5)°]. Both N(3)-C(10) bond distance 1.380(2)Å and N(6)-C(20) 1.372(2)Å bond distance are consistent with single bonds. This combined with the dihedral angles, [N(1), N(2), C(10)]∠[C(9), C(10), N(3)] = 56.2° and [N(4), N(5), C(20)]∠[C(19), C(20), N(6)] = 52.2°, indicate little π delocalization between outer nitrogen atoms and the NCN core. Bond distances around N(1), N(2) and C(10), and N(4), N(5) and C(20) average 1.338Å indicating partial double bonding character and a conjugated NCN core.

Interestingly, when **1** is heated to 100°C for 48 hours there was the formation of toluene peaks in the ^{1}H NMR spectrum of the reaction mixture. These new peaks can be accounted for by either an intramolecular elimination reaction involving the guanidine N-H and a benzyl group or a bimolecular reaction where a benzyl group from one molecule could come into contact with the N-H function of another molecule. From the NMR spectra it is difficult to say which is more likely since there is not a simple correlation in the decrease in integration of the N-H and the benzyl peaks.

An attempt to make a synthetically more versatile guanidinate complex lead us to consider the preparation of **2** (Equation 2). Two equivalents of neutral guanidine were added to zirconium tetrachloride with the anticipation that one equivalent of ligand would coordinate and a second equivalent would act as a base and react with any resulting HCl

forming complex **3**. Unfortunately, compound **2** was inseparable in any reasonable quantity from complex **3**. Only by repeated extractions with toluene was enough of complex **2** separated from the salt **3** to analyze by NMR studies. In an effort to indirectly confirm the identity of **2** by converting it to a more soluble product, a subsequent reaction was carried out using a reaction mixture of **2** and **3**. By assuming a 1:1 mole ratio of **2** and **3** as indicated in Equation 2, three equivalents of BzMgCl the expected product would contain one monoanionic guanidinate ligand bound to zirconium and three benzyl ligands. However, the resulting product **4** appeared by NMR spectra to posses two guanidinate ligands for every benzyl group. The formulation of **4** proposed in Equation 3 was consistent with these spectra.

Crystals of **4** suitable for x-ray analysis were easily obtained from toluene and used to confirm the spectroscopic results. Complex **4** crystallized in a distorted octahedral geometry with Cl and N(4) making up the axial positions [N(4)ZrCl 157.12(6)°]. The second guanidinate ligand is equatorial and the benzyl ligand (trans to N(2)) completes the coordination sphere. Both guanidine ligands exhibit similar features with N(6)-C(20) and N(3)-C(10) having single bond character with bond distances of 1.365(3)Å and 1.372(3)Å respectively. Both nitrogens are sp^2 hybridized with angles around N(6) and N(3) being 128.5(2)° and 125.6(2)°. However the dihedral angles, [N(1), N(2), C(10)]∠[C(10), N(3), C(7)] = 41.7° and [N(4), N(5), C(20)]∠[C(20), N(6), C(17)] = 33.5°, excludes the possibility of significant π overlap between N(6)-C(20) and N(3)-C(10). The difference of 8.2° is probably due to a steric effect rather than electronics. The N(2)-C(10) and N(1)-C(10) bond distances are consistent with partial double bond character (average = 1.342Å). Similarly N(5)-C(20) and N(4)-C(20) average 1.344Å. The Zr-Cl bond distance of 2.4744(7)Å is slightly longer than in $Zr[(CyN)_2CMe]_2Cl_2$ (Zr-Cl 2.431Å) and Cp_2ZrCl_2 (Zr-Cl 2.441Å).[4]

NMR studies show one benzyl (CH_2) peak and concur with the structural outcome that no η^2-coordination to the phenyl ring was present, thus making complex **4** a 12 electron species. The guanidinate bite angles N(2)ZrN(1) 59.56(7)° and N(4)ZrN(5) 60.56(7)° are also very similar to the zirconium amidinate complex, $Zr[(CyN)_2CMe]_2Cl_2$ (Bite angles 59.2(3)° and 60.3(3)°)[4] and to the other complexes reported throughout chapters 3 and 4.

One possible route to product **4** involves the use of two full equivalent of BzMgCl reacting complex **2** to form a dibenzyl version, then with the third equivalent the BzMgCl reacts with the hydrochloric salt **3** to form toluene and $MgCl_2$ and free ligand. This newly generated ligand would then be free to react with the dibenzyl version of **2** eliminating toluene in the process to finally give product **4**.

The third method of introduction explored in this chapter involved generation of anionic guanidinate by reaction with MeLi. This *in situ* generated dianion was allowed to react with $ZrCl_4$ with elimination of LiCl. In this case we attempted direct preparation of a dianionic guanidinate complex.

Spectroscopic investigation of **6** revealed three different and equal isopropyl methyl doublets. Such a pattern might be explained by a guanidine coordination in which a dianion has formed, thus making all isopropyl groups spectroscopically non-equivalent. A single crystal X-ray study was performed to help elicit the structural form of **6**.

Complex **6** is a dinuclear species possessing two bridging dianionic triisopropyl guanidine ligands. The molecule possesses a crystallographic inversion center. The nitrogen centers N(1) and the symmetry related N(1A) hold the dimer together by bridging the two zirconium atoms. The coordination geometry about each zirconium can best be described as tetrahedral based on the Zr-C(10) and Zr-C(10A) vectors and the two chloride ligands. Pertinent angles about zirconium are C(10)ZrCl(2) 119.15(16)°, Cl(2)ZrCl(1) 99.25(8)°

[Interestingly, the ClZrCl angle is significantly more open than in Cp_2ZrCl_2 where the ClZrCl angle is 97.12(2)°[4] and might be an important factor in polymerization reactions], Cl(1)ZrC(10A) 120.15(16)° and C(10A)ZrC(10) 89.0(2)° with the average being 106.9°. Bond distances N(3)-C(7) 1.500(9)Å and N(2)-C(4) 1.532(10)Å are consistent with single N-C bonds[5]. The bond distance N(2)-C(10) is 0.107Å longer than N(3)-C(10) but at the same time the corresponding N-Zr bond distances are essentially the same and about 0.2Å smaller than the N-C distances. This implies that one side of this molecule is skewed one way while the other symmetry-generated side is skewed in an equal and opposite fashion. There is no zirconium-zirconium interaction in this complex (Zr-Zr(A) 3.751Å).

An investigation of the catalytic properties of **6** has been initiated using the important co-catalyst MAO[6]. Upon addition of MAO (in a 1000:1 MAO:catalyst ratio) to a 100-ml toluene solution of **6** the reaction solution began to rapidly change color. Exposure of this system to ethylene gas resulted in an exothermic reaction with formation of a gelatinous solid in the reaction vessel. Filtration gave a white solid that was subsequently washed with acidic methanol to remove any present MAO or catalyst. The properties of the solid (melting point 122±5°C) are currently under investigation. Propylene gas addition caused only a mild exothermic reaction and no visible solid formed during the addition. However organic/inorganic extraction-purification techniques gave an organic soluble viscous liquid. This clear liquid was analyzed by EI MS giving a highest observed mass/charge value of 436 and a fragmentation pattern that was consistent with loss of C_3H_6 units. Solubility of the gelatinous liquid allowed for a 500 MHz HETCOR NMR in $CDCl_3$ experiment to be performed. The results are summarized in Table 5.

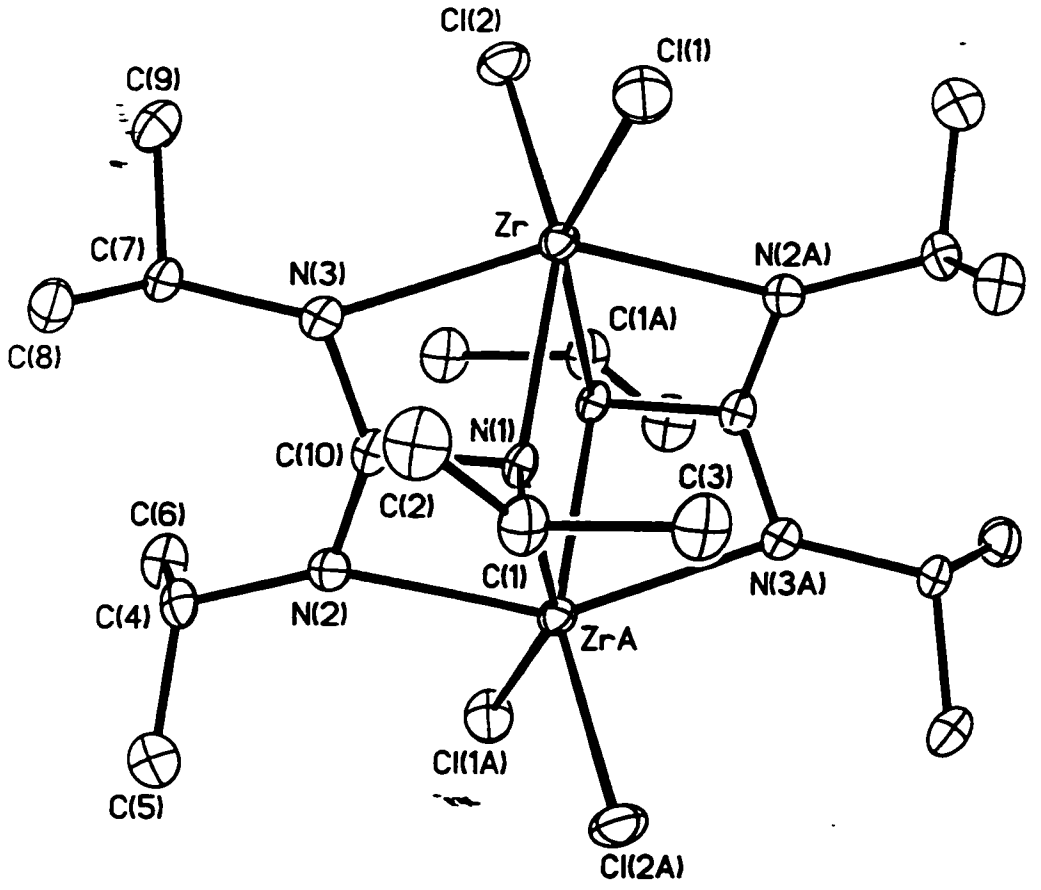

Figure 3. Molecular diagram for $[Cl_2Zr\{(^iPrN)_3C\}]_2$ (**6**). Thermal ellipsoids are drawn at 30% probability. Hydrogen atoms have been omitted for clarity.

Table 4. Bond distances and angles for $[Cl_2Zr\{(^iPrN)_3C\}]_2$ (**6**)

Bond distances					
Zr-N(3)	2.220(5)	Zr-N(1)A	2.253(5)	N(2)-C(4)	1.532(10)
Zr-N(2)A	2.267(6)	Zr-N(2)	2.282(6)	N(3)-C(10)	1.325(8)
Zr-Cl(1)	2.396(2)	Zr-Cl(2)	2.400(2)	C(10)-ZrA	2.630(7)
Zr-C(10)A	2.630(7)	Zr-C(10)	2.631(7)	N(2)-ZrA	2.267(6)
N(1)-C(10)	1.330(8)	N(1)-C(1)	1.502(8)	N(3)-C(7)	1.500(9)
N(1)-ZrA	2.253(5)	N(2)-C(10)	1.432(8)		
Bond angles					
N(3)-Zr-N(1)A	147.1(2)	N(3)-Zr-N(2)A	91.5(2)	C(10)-N(2)-C(4)	112.4(5)
N(1)A-Zr-N(2)A	60.18(19)	N(3)-Zr-N(2)	60.3(2)	C(4)-N(2)-ZrA	127.6(5)
N(1)A-Zr-N(2)	91.90(19)	N(2)A-Zr-N(2)	68.9(3)	C(4)-N(2)-Zr	117.5(4)
N(3)-Zr-Cl(1)	103.04(16)	N(1)A-Zr-Cl(1)	97.36(15)	C(10)-N(3)-C(7)	125.8(6)
N(2)A-Zr-Cl(1)	151.99(15)	N(2)-Zr-Cl(1)	97.59(16)	C(7)-N(3)-Zr	137.8(5)
N(3)-Zr-Cl(2)	94.00(16)	N(1)A-Zr-Cl(2)	107.93(16)	N(1)-C(1)-C(2)	109.6(6)
N(2)A-Zr-Cl(2)	103.50(17)	N(2)-Zr-Cl(2)	151.94(14)	C(6)-C(4)-N(2)	107.6(6)
Cl(1)-Zr-Cl(2)	99.25(8)	N(3)-Zr-C(10)A	117.2(2)	N(3)-C(7)-C(9)	106.5(6)
N(1)A-Zr-C(10)A	30.39(19)	N(2)A-Zr-C(10)A	32.96(19)	N(3)-C(10)-N(1)	138.9(6)
N(2)-Zr-C(10)A	70.2(2)	Cl(1)-Zr-C(10)A	120.15(16)	N(1)-C(10)-N(2)	110.2(6)
Cl(2)-Zr-C(10)A	118.67(17)	N(3)-Zr-C(10)	30.22(19)	N(1)-C(10)-ZrA	58.9(4)
N(1)A-Zr-C(10)	117.6(2)	N(2)A-Zr-C(10)	70.4(2)	N(3)-C(10)-Zr	57.5(4)
N(2)-Zr-C(10)	32.93(19)	Cl(1)-Zr-C(10)	111.92(17)	N(2)-C(10)-Zr	60.0(3)
Cl(2)-Zr-C(10)	119.15(16)	C(10)A-Zr-C(10)	89.0(2)	N(1)-C(10)-Zr	144.8(5)
C(10)-N(1)-C(1)	121.6(6)	C(5)-C(4)-N(2)	115.6(7)	ZrA-C(10)-Zr	91.0(2)
C(1)-N(1)-ZrA	142.5(4)	N(3)-C(7)-C(8)	114.0(6)	N(1)-C(1)-C(3)	108.8(6)
C(10)-N(2)-ZrA	87.6(4)	N(3)-C(10)-N(2)	110.1(6)	C(10)-N(1)-ZrA	90.7(4)
C(10)-N(2)-Zr	87.0(4)	N(3)-C(10)-ZrA	143.1(5)	C(10)-N(3)-Zr	92.3(4)
ZrA-N(2)-Zr	111.1(3)	N(2)-C(10)-ZrA	59.5(3)		

Typical polypropylenes have characteristic fingerprints that show peaks from 0.6-2.0 ppm. A broadened doublet at 0.84 ppm represents CH_3 groups, overlapping multiplets at 1.1 ppm represent CH_2 groups and 1.6 ppm represent CH groups.

Table 5. 500 MHz HETCOR NMR experiment on polypropylene[a]

^{13}C ppm	^{1}H ppm	^{13}C ppm	^{1}H ppm	^{13}C ppm	^{1}H ppm
47.7-45.9	0.8-1.2	29.7-22.2	Mult. at 1.6	20.6-19.2 1.0	mult. at 0.8
CH_2 groups		CH groups		CH_3 groups	

[a]One non correlated peak at 111.3 ppm in the ^{13}C can be assigned as a quaternary carbon

Preliminary results from this experiment suggest that it seems likely that complex **6** was able to polymerize propylene. Future work should involve studying the properties of the polyethylene and polypropylene polymers.

References

(1) Britovsek, G. J. P.; Gibson, V. C.; Wass, D. F. *Angew. Chem. Int. Ed.* **1999**, 38, 428

(2) Chandra, G.; Jenkins, A. D.; Lappert, M. F.; Srivastava, R. C. *J. Chem. Soc. (A)* **1970**, 2550

(3) Zucchini, U.; Albizzati, E.; Giannini, U. *J. Organometal Chem.* **1971**, 26, 357

(4) Littke, A.; Sleiman, N.; Bensimon, C.; Richeson, D. S.; Yap, G. P. A.; Brown, S. *Organometallics* **1998**, 17, 446

(5) Patai, S. *The chemistry of amidines and amidinates*, John Wiley & Sons, Toronto, **1975**, Chapter 1

(6) (a) Scollard, J. D.; McConville, D. H. *J. Am. Chem. Soc.* **1996**, 118, 10008

(b) Christoffers, J.; Bergman, R. G. *J. Am. Chem. Soc.* **1996**, 118, 4715

(c) Bochmann, M. *J. Chem. Soc. Dalton Trans.* **1996**, 255

General Thesis Conclusions

One of the central themes in this thesis was to develop general routes to guanidinate complexes of early transition metals and to investigate ligand-metal bonding interactions. Two guanidine ligands were employed in this quest.

Steric interactions on the third nitrogen atom and their effect on ligand electronics were discussed in chapter one and are represented in Scheme 3 of chapter one. A concern raised was that the bulky tetra-substituted ligand might encourage a large dihedral angle, to relieve steric hindrance, and discourage the appropriate orientation for π conjugation. This was indeed the case as the tetra substituted guanidinate ligand was found to bind with the $N(SiMe_3)_2$ groups in a near perpendicular arrangement with respect to the planar MNCN function. This orientation was rationalized to be a result of steric hindrance. This arrangement excluded any significant contribution from the zwitterionic form of the ligand. Varying the R (Cy or ^{i}Pr) groups on the core nitrogen atoms seemed to add little to the overall sterics of the system.

Reducing the sterics on this third nitrogen by replacing the trimethylsilyl groups with a single, smaller isopropyl group did tend to give complexes with more C-N double bond character and smaller dihedral angles, however only in certain complexes were the dihedral angles small enough to say that some dianionic character might be present.

Electronically the two ligands seem to be different from each other. Evidence for the tri-alkyl substituted guanidinate ligand being a better electron donors than the trimethylsilyl groups on the tetra substituted guanidinate ligand was provided by comparing benzyl structures. The tetra substituted guanidinate complex with three benzyls show that the phenyl group is a weak electron donor (η^2 bonding). This might indicate that the trimethylsilyl

substituent is slightly electron withdrawing versus alkyl groups in the tri-substituted guanidinate complex where no η^2 bonding was found.

Different supporting ligands had a dramatic effect on the mode of tri-substituted guanidinate coordination. Strong π donating ligands such as dimethylamide groups reduce the electron deficiency of the metal and so disfavours a η^3 coordination mode of the ligand. However, amide groups tend to favour a dianionic state. The sensitivity of which coordination mode is favoured was further demonstrated when an amide group was replaced with a chloride ligand. In this case the guanidinate ligand preferred a monoanionic state. As we move to ligands that lack any π donating possibilities, i.e. alkyl groups, it is found that a complex with four methyl groups preferred monoanionic guanidinate coordination. This is in contrast to dianionic coordination when three dimethylamide groups were present. In addition to this, a trend leading to larger dihedral angles and longer C-N bonds was found when chloride ligands were replace by alkyl groups. This effect leads to reduced π overlap within the ligand which would be necessary to form a fully conjugated system containing a dianionic ligand. A similar trend for group four complexes was noticed when a benzyl ligand replaced a chloride ligand and caused the dihedral angle to increase significantly. When a system containing only chloride supporting ligands was used a dianionic ligand resulted. However in this case a bridging mode was adopted. From these results it appears that chloride ligands could be the best choice as supporting ligands if a dianionic guanidine ligand is sought. Chloride ligands are also perhaps the most versatile supporting ligands since many replacement reactions can be performed on them. However, a major problem is that guanidinate complexes with metal chloride ligands seem to lack good solubility in typical organic solvents and so purification is difficult.

The tri-substituted ligand had the potential to yield a dianionic species by deprotonation of a second N-H function, however, it seems that alkyl groups on the metal are strong enough bases to deprotonate one N-H, but not both. Investigations involved in converting these monoanionic complexes to their dianionic form have so far been unsuccessful, as significant decomposition has been observed.

Perhaps the best method of introduction of a dianionic guanidinate ligand to a metal involves the reaction of a dilithium salt of the ligand reacting with a metal chloride. This method was proven useful in chapter four. Preliminary reactivity studies show that the decomposition problem, involved when reactions on the monoanionic complexes are performed, is not as common or important.

Further work should concentrate on reactions using this dilithium salt with other metal halides to determine if this is a general method of guanidinate introduction as well as study the resulting binding modes as complexes are made from various transition metal groups.